



بسم الله الرحمن الرحيم

Sudan University of Science and Technology



Faculty of Engineering

Department of biomedical Engineering

**Reduction Of Speckle Noise And Image Enhancement
In Ultrasound Image Using Filtering Technique And
Edge Detection.**

تقليل ضوضاء الرقطة وتحسين صورة الموجات الصوتية باستخدام تقنية
المرشحات مع كاشف الحواف

Prepared By:

- Etimad Alhady Mustafa Mohammed Ahmed .
- Arwa Abdalgader Mohmmmed Ahmed Sanad .
- Islam AbdElmutalab Hassan Mohmed .

Supervised By:

Dr.Banazier Ahmed Abraham

2017

قال تعالى: (35) "اللَّهُ نُورُ السَّمَاوَاتِ
وَالْأَرْضِ مَثَلُ نُورِهِ كَمِشْكَاةٍ فِيهَا مِصْبَاحٌ الْمِصْبَاحُ فِي
رُجَاةٍ الزَّجَاةِ كَأَنَّهُا كَوْكَبٌ دُرِّيٌّ يُوقَدُ مِنْ شَجَرَةٍ مَبَارَكَةٍ
زَيْتُونَةٍ لَّا شَرْقِيَّةٍ وَلَا غَرْبِيَّةٍ يَكَادُ زَيْتُهَا يُضِيءُ وَلَوْ لَمْ
تَمْسَسْهُ نَارٌ نُّورٌ عَلَى نُورٍ يَهْدِي اللَّهُ لِنُورِهِ مَن يَشَاءُ
وَيَضْرِبُ اللَّهُ الْأَمْثَالَ لِلنَّاسِ وَاللَّهُ بِكُلِّ شَيْءٍ
عَلِيمٌ" (36)

سورة النور الآية (35)-(36)

Dedication

This project is dedicated to our beloved parents ,sisters ,brothers and teacher, whose support us as they can; educated us and enabled us to reach at this level.

Acknowledgment

Thanks to Allah at firstly ,the lord of the worlds ,for his mercy and limitless help and guidance .my peace and blessings be upon Mohamed the last of messengers .

secondly we would like to express gratitude to supervisor Dr . Banazier Ahmed Abrahams not also for giving us support not only in technical problems solving ,but also moral support for the beginning of the project until the a accomplishment of the project ,and all her help guidance, her patience valuable encouragement during this study .Also would like to express thanks to the staff members in the department of biomedical engineer- Al- Sudan University. Also, heartily thankful our teachers and friends whose support us in this project.

Table of contents

	Content	Pg.No
	Dedication	I
	Acknowledgment	Ii
	Table of content	Iii
	List of table	vi
	List of figure	vii
	Abbreviation	X
	Abstract	xi
	المستخلص	Xii

Chapter one: introduction

1.1	General review	1
1.2	problem of the statement	1
1.3	General objective	1
1.4	specific objective	2
1.5	Methodology	2
1.6	thesis layout	2

Chapter two: Theoretical Background

2.1	Waves	3
2.2	Sound waves	3
2.2.1	Categories of sound	3
2.3	What is ultrasound?	3
2.3.1	Basic of ultrasound	4
2.3.2	Echolocation	4
2.3.3	Ultrasound safety	4
2.4	Ultrasound modes	4
2.5	Ultrasound's interaction with the medium	5
2.5.1	Reflection	7
2.5.2	Scattering	7

2.5.3	Attenuation	7
2.5.4	Absorption	8
2.6	Ultrasound Imaging System	8
2.7	Introduction to ultrasound	9
2.8	Speckle noise in ultrasound imaging:	9
2.9	Pattern of Speckle Noise	10
2.10	Need for despeckling	11
2.11	Speckle reduction methods	11
2.11.1	Compounding methods	11
2.11.2	Post-acquisition method	11
2.11.2.1	Single scale spatial filtering method	11
2.11.2.2	Multi scale method	12
2.11.2.2.1	Wavelet based speckle reduction method	12
2.11.2.2.2	Pyramid based speckle reduction method	12
2.12	Speckle model	13
2.13	Despeckling filter	14
2.13.1	Homogenous mask filtering	14
2.13.2	Median filter	14
2.13.3	Linear scaling filter r	15
2.13.4	Geometric filtering	15
2.13.5	Anisotropic diffusion filtering	15
2.13.6	Wavelet filtering	15
2.13.7	Total variation denoising	16
2.14	Limitation of despeckle filtering techniques	16
2.15	Image quality evaluation metrics	17
2.16	Edge detection	18

2.16.1	Canny operator	19
2.16.2	sobel operator	19
2.16.3	Prewitt operator	20
2.16.4	Robert operator	20
2.16.5	Laplacian operator	21

Chapter three: literature review

Chapter four: materials and methodology

4.1	materials and methodology	26
4.2	proposed method algorithm	26

Chapter five: result and desiccation

5.1	Experimental result	28
-----	---------------------	----

Chapter six: conclusion and future work

6.1	Conclusion	86
6.2	Recommendation	87

List of table

Table 5.1	Image quality evaluation metrics computed for the Liver ($\sigma = 0.5$) at statistical measurement of RMSE, SNR and SSIM for different filter types.
Table 5.2	Image quality evaluation metrics computed for the Liver ($\sigma = 0.05$) at statistical measurement of RMSE, SNR and SSIM for different filter types.
Table 5.3	Image quality evaluation metrics computed for the kidney($\sigma = 0.5$) at statistical measurement of RMSE, SNR and SSIM for different filter types.
Table 5.4	Image quality evaluation metrics computed for the kidney($\sigma = 0.05$) at statistical measurement of RMSE, SNR and SSIM for different filter types.
Table 5.5	Image quality evaluation metrics computed for the fetal ($\sigma = 0.5$) at statistical measurement of RMSE, SNR and SSIM for different filter types.
Table 5.6	Image quality evaluation metrics computed for the fetal ($\sigma = 0.05$) at statistical measurement of RMSE, SNR and SSIM for different filter types.
Table 5.7	Image quality evaluation metrics computed for the liver edge detection operators ($\sigma = 0.5$) at statistical measurement of RMSE, PSNR SNR and SSIM for different filter types.
Table 5.8	Image quality evaluation metrics computed for the liver edge detection operators($\sigma = 0.05$) at statistical measurement of RMSE,PSNR SNR and SSIM for different filter types.
Table 5.9	Image quality evaluation metrics computed for the kidney edge detection operators($\sigma = 0.5$) at statistical measurement of RMSE, ,PSNR SNR and SSIM for different filter types.
Table 5.10	Image quality evaluation metrics computed for the kidney edge detection operators ($\sigma = 0.05$) at statistical measurement of RMSE,PSNR SNR and SSIM for different filter types.

Table 5.11	Image quality evaluation metrics computed for the fetal edge detection operators ($\sigma= 0.5$) at statistical measurement of RMSE,PSNR SNR and SSIM for different filter types.
Table 5.12	Image quality evaluation metrics computed for the fetal edge detection operators($\sigma=0.05$) at statistical measurement of RMSE ,PSNR SNR and SSIM for different filter types.
Table5.13	Image quality evaluation metrics computed Hyperid technique by use Linear Scaling Filtering(FCA) , Anisotropic Diffusion Filtering(Rad)and Linear Scaling(NeighborHood Averaging) Filtering (sort) statistical measurement of RMSE,PSNR ,SNR and SSIM.
Table5.14	Image quality evaluation metrics computed Hyperid technique by use Linear Scaling Filtering(FCA) , Anisotropic Diffusion Filtering(Rad)and Linear Scaling(NeighborHood Averaging) Filtering (sort) statistical measurement of RMSE,PSNR ,SNR and SSIM.

List of figure

Figure2.1	Ultrasound's Interaction with the medium.	
Figure 2.2	Block diagram of Ultrasound Imaging System.	
Figure 4.1	Flow chart for proposed method.	
Figure5.1	Results of liver despeckled by various filter on multiplication noise ($\sigma_n=0.5$).	
Figure5.2	Histogram result of liver despeckled by various filter on multi active noise(noise =0.5).	
Figure5.3	Performance analysis graph to image quality evaluation metric for liver image (noise $\sigma_n =0.5$).	
Figure5.4	Results of liver despeckled by various filter on multiplication noise ($\sigma_n=0.05$).	
Figure5.5	Histogram result of liver despeckled by various filter on multi active noise(noise =0.05).	
Figure5.6	Performance analysis graph to image quality evaluation metric for liver image (noise $\sigma_n =0.05$).	
Figure5.7	Results of kidney despeckled by various filter on multiplication noise ($\sigma_n=0.5$).	
Figure5.8	Histogram result of kidney despeckled by various filter on multi active noise(noise =0.5)	
Figure5.9	Performance analysis graph to image quality evaluation metric for kidney image (noise $\sigma_n =0.5$).	
Figure5.10	Results of kidney despeckled by various filter on multiplication noise ($\sigma_n=0.05$).	
Figure5.11	Histogram result of kidney despeckled by various filter on multi active noise(noise =0.05)	
Figure5.12	Performance analysis graph to image quality evaluation metric for kidney image (noise $\sigma_n =0.05$).	
Figure5.13	Results of fetal despeckled by various filter on multiplication noise ($\sigma_n=0.5$).	
Figure5.14	Histogram result of fetal despeckled by various filter on multi active noise(noise =0.5)	
Figure5.15	Performance analysis graph to image quality evaluation metric for fetal image (noise $\sigma_n =0.5$).	

Figure5.16	Results of fetal despeckled by various filter on multiplication noise ($\sigma=0.05$)	
Figure5.17	Histogram result of fetal despeckled by various filter on multi active noise(noise =0.05)	
	Post processing	
Figure5.18	result of various edge detection operators for original liver image.	
Figure5.19	histogram result of various edge detection operators for original liver image.	
Figure5.21	result of various edge detection operators for despeckling liver image DSFRAD (σ 0.5).	
Figure5.22	histogram result of various edge detection operators for despeckling liver image DSFRAD (σ 0.5).	
Figure5.23	result of various edge detection operators for despeckling liver image DSFRAD (σ 0.05) with.	
Figure5.24	histogram result of various edge detection operators for despeckling liver image DSFRAD (σ 0.05) .	
Figure5.25	result of various edge detection operators to original kidney image.	
Figure5.26	result of various edge detection operators to original kidney image.	
Figure5.27	result of various edge detection operators for despeckling kidney image DSFRAD (σ 0.5) .	
Figure5.28	histogram result of various edge detection operators for despeckling kidney image DSFRAD (σ 0.5) .	
Figure5.29	result of various edge detection operators todespeckling kidney image DSFRAD (σ 0.05)	
Figure5.30	histogram result of various edge detection operators for despeckling kidney image DSFRAD (σ 0.05) .	
Figure5.31	result of edge detection operators of original fetal image.	

Figure5.32	histogram result of various edge detection operators for fetal image.	
Figure5.33	result of various edge detection operators for despeckling fetal image DSFRAD ($\sigma_n 0.5$) .	
Figure5.34	histogram result of various edge detection operators for despeckling fetal image DSFRAD ($\sigma_n 0.5$) .	
Figure5.35	result of various edge detection operators for despeckling fetal image DSFRAD ($\sigma_n 0.05$).	
Figure5.36	histogram result of various edge detection operators for despeckling fetal image DSFRAD ($\sigma_n 0.05$).	
Figure5.37	Result image Hyperid technique by use Linear Scaling Filtering.	
Figure5.38	Result image Hyperid technique with Linear Scaling(NeighborHood Averaging)Filtering	
Figure5.39	Result image Hyperid technique by use Anisotropic Diffusion Filtering Filtering	

Abbreviation

US	Ultrasound
US B-mode	Ultrasound Brightness mode
US A-mode	Ultrasound Amplitude mode
US M-mode	Ultrasound Motion mode
SND	Scatter Number Density
FFS	Fully Formed Speckle pattern
NRLR	Non Randomly distributed with Long-Range
NRSR	Non Randomly distributed with Short-Range order
PDF	Probability Density Function
DsFgf4d	Geometric Filter
SRAD	Speckle reduction anisotropic diffusion
TV	Total Variation
RMSE	Root Mean Square Error
SNR	Signal to Noise Ratio
PSNR	Peak Signal to Noise Ratio
SSIM	Structural Similarity Index
DsFlecasort	Linear scaling and sorting despeckle filter
IQMs	Image quality metrics
DsFlsminsc	Minimum speckle index homogeneous mask despeckle filter
DsFmedian	Median despeckle filter
TV	Television
DsFwaveltc	Wavelet despeckle filter
2D	Two-dimensional
3D	Three-dimensional
SAR	Synthetic aperture radar
DsFca	Linear scaling of the gray-level despeckle filter
SO_SORT	Sobel _ Linear scaling and sorting despeckle filter

المستخلص

جهاز الموجات فوق الصوتية تطبيقاته واسعة في مجال التصوير الطبي وغيرها من المجالات . له العديد من المزايا التي يتفوق بها على طرق التصوير الطبي الأخرى . يستخدم جهاز الموجات الصوتية في التشخيص بصورة أساسية وذلك يعود إلى أن استخدامه سطحي ,محمول ,دقيق , تكلفته منخفضة ,قدرته على تشكيل صورة في الوقت الحقيقي و الاستمرار في تحسين جودة الصورة تشير التقديرات إلى ان كل شكل من أشكال الدراسات الطبية التشخيصية صورة في العالم ينطوي على تقنيات الموجات فوق الصوتية .

الهدف من هذه الرسالة هو إعطاء لمحة عامة عن أنواع تقنيات رقطة الحد في التصوير جهاز الموجات الصوتية وتقديم تقنية جديدة للحد من البقع والقيام تصفية التصفية استنادا إلى مقاييس جودة الصورة وهناك طريقة جديدة مقترحة لتقليل الرقطة وتعزيز تماسك الصورة الطبية :

تم استخدام تسعة مرشحات وخمسة عمليات كاشف حواف وتم تقييم جودة الصورة ,معايير جودة الصورة وجدت ان الطريقة المقترحة افضل من الطرق الاخرى , حيث ان التفاصيل التركيبية تحافظ على ملامح الصورة المهمة التي على معلومات تشخيصية بافضل طريقة مقارنة بالمرشحات الاخرى .

ABSTRACT

ultrasound (us) imaging application in medicine and other fields is enormous .it has several advantages over other medical imaging modalities .the use of us in diagnosis is well established because of noninvasive nature , portable ,accurate ,low cost imaging modality , capability of forming real time imaging and continuing improvement in image quality .it's estimated that one out of every form medical diagnostic image studies in the world involves ultrasonic techniques .the objective of this thesis is to give an overview about types of speckle reduction techniques in US imaging and to present new technique of speckle reduction and to carry out comparative evaluation of despeckle filtering based on image quality metrics .

A new speckle suppression method and coherence enhancement of medical US image where proposed: Nine despeckled filtering techniques and five edge detection operators ,the result evaluated by image quality metrics; then best edge detection hybrid with best filter , quality evaluation metrics has been found that the proposed method performance better than all other methods, while the structural details and result preserving of small and important image feature that contain diagnostic information in a better way than other despeckling filter.

1.1 General review

medical images are widely used and usually corrupted by noise in its acquisition and transmission. The main objective of image denoising technique is necessary to remove such noises while retaining as much as possible the important signal features. Ultrasonic imaging procedure because it's economical, comparatively safe, transferable and adaptable, though one of its one shortcoming is poor quality of image which are affected by speckle noise. The existence of speckle is unattractive since it disgraces image quality and it affects the tasks of individual interpretation and diagnosis accordingly. Speckle filter is a central preprocessing step for feature extraction, analysis and recognition from medical imagery measurements. Previously a number of filters have been proposed for speckle mitigation ratio while conserving the edge and lines in the image. [7]

1.2 problem statement

Ultrasound imaging is a widely used and safe medical diagnostic technique, due to its noninvasive nature, portable, accurate, low cost imaging modality, capability of forming real time imaging and continuing improvement in image quality.

Unfortunately, the quality of ultrasound images (as defined by image resolution and contrast) is generally limited due to a number of factors, speckle noise. The speckle noise is multiactive noise so it is difficult to remove it than additive noise. Speckle noise is considered as an effective problem in US image so that we need to process it with preserving of small and important image features that contain diagnostic information.

1.3 General objective

In this research a total of 9 speckle filters were used and the best filter for speckle noise reduction in medical ultrasound images was selected by using image quality metrics evaluation; then 5 edge detection operators were selected and the best edge detection, Hybrid technique was evaluated by IQMS and the best filter to preserve of small and important image features was selected.

1.4 Specific objective

The objective of this research is to give an overview about type of hybrid speckle reduction technique and to carry out the comparative evaluation of . The speckle noise is multiactive noise so it difficult to remove it than additive noise . Speckle noise is considered as effective filter that perceive edge detection and comparative by image quality evaluation metrics with original image.

1.5 Methodology

Images from IBE Tech(Giza . Egypt) database of ultrasound image including Liver and fetal , ultrasound scanmalaysia.com including kidney. In the quantitative study Adding speckle noise with different variance on ultrasound images and using most importantly technique to removing that noise .

Hybrid technique

This proposed technique is hybrid between best edge detection and best filter; image quality evaluation metrics was found to compare the performance of this hybrid technique.

1.6thesislayout

The layout of this thesis consist of six chapters there are: chapter one include introduction, while chapter two involve theoretical background, literature review in chapter three , in chapter four materials and methodology, however in chapter five the results and discussion were viewed , finally chapter six is conclusion and future work.

2.1 Wave

There are two types of waves: Transverse waves: these waves are perpendicular to the direction of energy transfer, e.g., violin string. Longitudinal waves: these waves are parallel to the direction of energy transfer, e.g., a pulse from a piston in a cylinder, sound waves. [1]

2.2 Sound waves

Sound wave propagate by longitudinal motion (compression/expansion) but not transverse motion (side-to-side) Can be modeled as weights connected by springs. [2]

2.2.1 Categories of sound

Audible sounds (20_2000Hz) such as:

Sonic sounds.

Non - audible sounds such as:

Ultrasonic waves (higher than 20000Hz) and the infrasonic waves (less than 20Hz).[3]

2.3 What is Ultrasound?

Is Acoustic waves are mechanical pressure waves. Ultrasound waves are pressure waves that travel through a medium at a frequency greater than 20 kHz.

1. Humans can typically hear frequencies between (20 Hz to 20 kHz).
2. Children can detect higher frequencies than adults.
3. Animals
 - Many animals can detect higher frequencies
 - Dogs – up to 22 kHz
 - Fish – up to 180 kHz
4. Other animals detect lower frequencies

Infrasound – below 20 Hz

5. Attenuation vs Resolution

Higher frequency has smaller wavelength $c = f\lambda$.

Better spatial resolution.

Higher frequency waves degrade faster with distance.

Trade-off between penetration depth and spatial resolution. [4]

2.3.1 Basics of Ultrasound

Propagation of ultrasound waves are defined by the theory of acoustics. Ultrasound moves in a wavelike fashion by expansion and compression of the medium through which it travels.

Ultrasound waves travel at different speeds depending on material and can be absorbed, refracted, focused, reflected, and scattered.

Process Overview:

A. Transducer (electrical signal a acoustic signal) generates pulses of ultrasound and sends them in to patient.

B. Organ boundaries and complex tissues produces echoes (reflection or scattering) which are detected by the transducer.

C. Echoes displayed on a grayscale anatomical image

Each point in the image corresponds to an anatomical location of an echo generating structure.

Brightness corresponds to echo strength. [4]

2.3.2 Echolocation

1. “Biosonar” or “Active navigation”. 2. Animals emit sounds and listen for echoes: Used to navigate or to hunt. Bats, toothed whales and dolphins, shrews, and cavedwelling birds use biosonar. Ultrasound, audible, and infrasound frequencies. Many other animals use “passive” biosonar. 3. Humans: Listening is equivalent to passive biosonar. [4]

2.3.3 Ultrasound Safety

A. High intensity ultrasound causes heating.

B. Could damage body tissues. C. Low intensity ultrasound is always used for diagnostics. [4]

2.4 Ultrasound modes

The two main scanning modes are A- and B-modes. Other modes used are M mode, duplex ultrasound, color-coded ultrasound, and power Doppler ultrasound, which will be briefly introduced below.

A-mode refers to amplitude mode scanning, which is mainly of historical interest. In this mode, the strength of the detected echo signal is measured and displayed as a continuous signal in one direction. A-mode is a line, with strong reflections being represented as an increase in the signal amplitude. This scanning technique has the limitation that the recorded signal is 1D with limited anatomical information. A mode is no longer used, especially for the assessment of cardiovascular disease. Its use is restricted to very special uses such as in ophthalmology to perform very accurate measurements of distance.

B-mode refers to the brightness mode. In B-mode, echoes are displayed as a 2D gray scale image. The amplitude of the returning echoes is represented as dots (pixels) of an image with different gray values. Advances in B-mode ultrasound have resulted in improved anatomic definition, which has enabled plaque characterization.

M-mode is used in cardiology, and it is actually an A-scan plotted against time. The result is the display of consecutive lines plotted against time. Using this mode, detailed information may be obtained about various cardiac dimensions and also the accurate timing of vascular motion.

D-mode (D=Doppler) this imaging mode is based on the Doppler Effect, i.e. change in frequency (Doppler shift) caused by the reciprocal movement of the sound generator and the observer. Diagnostic ultrasound uses the change in frequency of ultrasound signal backscattered from red blood cells. The frequency of the reflected ultrasound wave increases or decreases according to the direction of blood flow in relation to the transducer. [9]

2.5 Ultrasound's Interaction with the medium

The interaction between the medium and the ultrasound emitted into the medium can be described by the following phenomena: The echo that travels back to the transducer and thus gives information about the medium is due to two phenomena: reflection and scattering. Reflection can be thought of as when a billiard ball bounces off the barrier of the table, where the angle of reflection is identical to the angle of incidence. Scattering (spreading) can be thought of, when one shines strong light on the tip of a needle: light is scattered in all directions.[9] In acoustics, reflection and scattering is taking place when the emitted pulse is travelling through the interface between two media of different acoustic properties, as when hitting the interface of an object with different acoustic properties. Specifically, reflection is taking

place when the interface is large relative to the wavelength (e.g. between blood and intima in a large vessel). Scattering is taking place when the interface is small relative to the wavelength (e.g. red blood cell). The abstraction of a billiard ball is not complete, however: In medical ultrasound, when reflection is taking place, typically only a (small) part of the wave is reflected. The remaining part is transmitted through the interface. This transmitted wave will nearly always be refracted, thus typically propagating in another direction. The only exception is when the wave impinges perpendicular on a large planar interface: The reflected part of the wave is reflected back in exactly the same direction as it came from (like with a billiard ball) and the refracted wave propagates in the same way as the incident wave.

Reflection and scattering can happen at the same time, for instance, if the larger planar interface is rough. The smoother, the more it resembles pure reflection (if it is completely smooth, specular reflection takes place). The rougher, the more it resembles scattering.

When the emitted pulse travels through the medium, some of the acoustic (mechanical) energy is converted to heat by a process called Absorption. Of course, also the echoes undergo absorption.

Finally, the loss in intensity of the forward propagating acoustic pulse due to reflection, refraction, scattering and absorption is under one named attenuation. [9]

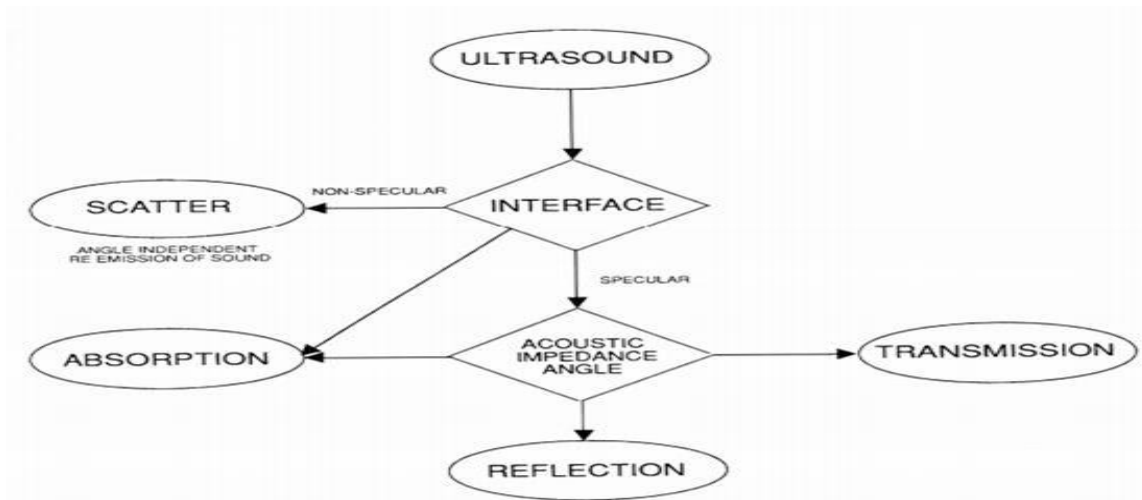


FIGURE2.1: Ultrasound’s Interaction with the medium. [7]

2.5.1 Reflection

When a plane wave impinges on a plane, infinitely large, interface between two media of different acoustic properties, reflection and refraction occurs meaning that part of the wave is reflected and part of the wave is refracted. The wave thus continues its propagation, but in a new direction. In the human body, approximate reflection can be observed at the interface between blood and the intima of large vessel walls or at the interface between urine and the bladder wall. [7]

2.5.2 Scattering

While reflection takes place at interfaces of infinite size, scattering takes place at small objects with dimensions much smaller than the wavelength. Just as before, the specific acoustic impedance of the small object must be different from the surrounding medium. The scattered wave will be more or less spherical, and thus propagate in all directions, including the direction towards the transducer. The latter is denoted backscattering. [7]

2.5.3 Attenuation

the loss of intensity (or energy) of the forward propagating wave due to reflection, refraction, scattering and absorption is denoted attenuation. The intensity is a measure of the power through a given cross-section; thus the units are W/m². It can be calculated as the product between particle velocity and pressure:

$$I = \rho v = p^2 / Z \quad (2.1)$$

Where Z is the specific acoustic impedance of the medium. If I (0) is the intensity of the pressure wave at some reference point in space and I (x) is the intensity at a point x further along the propagation direction then the attenuation of the acoustic pressure wave can be written as:

$$I = I(0)e^{-\alpha x} \quad (2.2)$$

Where α (in units of m^{-1}) is the attenuation coefficient. α depends on the tissue type (and for some tissue types like muscle, also on the orientation of the tissue fibers) and is approximately proportional with frequency. [7]

2.5.4 Absorption

Absorption is the conversion of acoustic energy into heat. The mechanisms of absorption are not fully understood, but relate, among other things, to the friction loss in the springs, mentioned in Subsection pure absorption can be observed by sending ultrasound through a viscous liquid such as oil. [7]

2.6 Ultrasound Imaging System

Figure 2.2 shows a functional block diagram of an ultrasound imaging system. The construction of ultrasound B-mode image involves capturing the echo signal returned from tissue at the surface of piezoelectric crystal transducers. These transducers convert the ultrasonic RF mechanical wave into electrical signal. Convex ultrasound probes collect the echo from tissue in a radial form. Each group of transducers is simultaneously activated to look at a certain spatial direction from which they generate a raw line signal (stick) to be used later for raster image construction. These sticks are then demodulated and logarithmically compressed to reduce their dynamic range to suit the commercial display devices. The final Cartesian image is constructed from the sampled sticks in a process called scan conversion.

Speckle reduction techniques can be applied on envelope detected data, log compressed data or on scan converted data. However, slightly different results will be produced for each data. In the compression stage some useful information about the imaged object may be deteriorated or even lost. However, any processing which works with envelope detected data has more information at its disposal and preserves more useful information. Compared to processing the scan converted image, envelope detected data has fewer pixels and thus incurs lower computational cost.

For optimum result envelope detected data processing is preferred because some information that lost after the compression stage cannot be recovered by working with log compressed data or the scan converted image. However, the real time speckle reduction methods are applied on the scan converted image, since the scan converted image is always accessible where most commercial ultrasound systems do not output the envelope detected or log compressed data. [5]

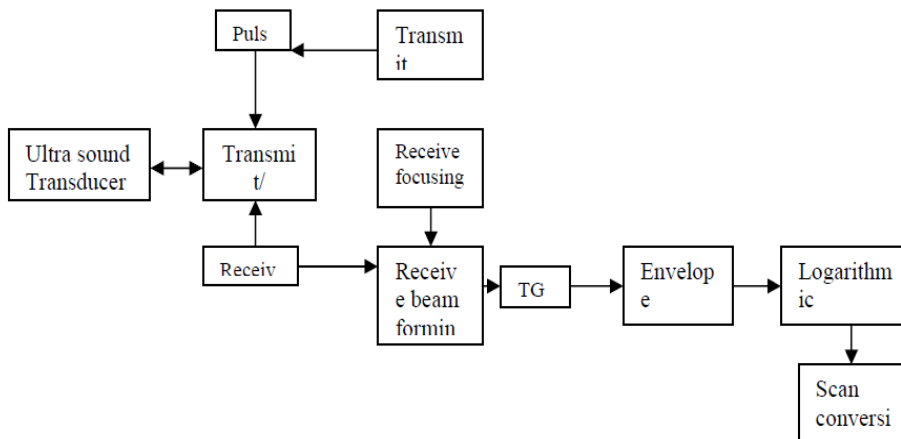


FIGURE 2.2: Block diagram of Ultrasound Imaging System. [5]

2.7 Introduction of ultrasound

Ultrasound imaging system is widely used diagnostic tool for modern medicine. It is used to do the visualization of muscles, internal organs of the human body, size and structure and injuries. Obstetric sonography is used during pregnancy. In an ultrasound imaging speckle noise shows its presence while doing the visualization process. Medical images, Satellite images are usually degraded by noise during image acquisition and transmission process. The main purpose of the noise reduction technique is to remove speckle noise by retaining the important feature of the images. In this research digital image processing is suitable for solving this problem. The main concern is digital image processing which involves using a computer to change nature of digital images. Digital image processing uses the computer algorithms to perform image processing on digital images. Noise removal and edge detection and the two most important steps in processing of any digital images for improving the information in the picture so that it can be easily understand by human and to make it suitable and readable for any machine which works on those images. [5]

2.8 Speckle in Ultrasound Imaging

Speckle in US B-scans is seen as a granular structure which is caused by the constructive and destructive coherent interferences of back scattered echoes

from the scatterers that are typically much smaller than the spatial resolution of medical ultrasound system. This phenomenon is common to laser, sonar and synthetic aperture radar imagery (SAR). Speckle pattern is a form of multiplicative noise and it depends on the structure of imaged tissue and various imaging parameters. Speckle degrades the target detectability in B-scan images and reduces the contrast, resolutions which affect the human ability to identify normal and pathological tissue. It also degrades the speed and accuracy of ultrasound image processing tasks such as segmentation and registration. [5]

2.9 Pattern of Speckle Noise

The nature of the speckle pattern can be categorized into one of three classes according to the number of scatterers per resolution cell or the so called scatter number density (SND), spatial distribution and the characteristics of the imaging system itself. These classes are described as follows:

1. FFS (Fully formed speckle) pattern, which occurs when many fine randomly distributed scattering sites exist within the resolution cell of the pulse-echo system. In this case, the amplitude of the backscattered signal can be modeled as a Rayleigh distributed random variable with a constant SNR of 1.92. Under such conditions, the textural features of the speckle pattern represent a multivariate signature of the imaging instrument and its point spread function. Blood cells are typical examples of this type of scatterers.
2. Non randomly distributed with long-range order (NRLR). Examples of this type are the lobules in liver parenchyma. It contributes a coherent or specular backscattered intensity that is in itself spatially varying. Due to the correlation between scatterers, the effective number of scatterers is finite . This situation can be modeled by the K-distribution. This type is associated with SNR below 1.92. It can also be modeled by the Nakagami distribution.
3. Non randomly distributed with short-range order (NRSR). Examples of this type include organ surfaces and blood vessels. When a spatially invariant coherent structure is present within the random scatterer region, the probability density function (PDF) of the backscattered signals becomes close to the Rician distribution. This class is associated with SNR above 1.92. [5]

2.10 Need for despeckling

speckle is considered as the dominant source of noise in ultrasound imaging and should be processed without affecting important image features. The main purposes for speckle reduction in medical ultrasound imaging are:

- 1.To improve the human interpretation of ultrasound images-speckle reduction makes an ultrasound image cleaner with clearer boundaries.

- 2.Despeckling is a preprocess step for many ultrasound image processing tasks such as segmentation and registration – speckle reduction improve the speed and accuracy of automatic and semiautomatic segmentation & registration. [5]

2.11Speckle reduction methods

Several techniques have been proposed for despeckling in medical ultrasound imaging. In this section we present the classification and theoretical overview of existing despeckling techniques. [5]

2.11.1Compounding methods

In this method a series of ultrasound images of the same target are acquired from different scan directions and with different transducer frequencies or under different strains .Then the images are averaged to form a composite image. The compounding method can improve the target detectability but they suffer from degrade spatial resolution and increased system complexity. [5]

2.11.2 Post Acquisition Methods

This method do not require many hardware modification .The post acquisition image processing technique falls under two categories (1)Single scale spatial filtering (2) Multiscale Methods. [5]

2.11.2.1 Single Scale spatial filtering

A Speckle reduction filter that changes the amount of smoothing according to the ratio of local variance to local mean was developed. In that method

smoothing is increased in homogeneous region where speckle is fully developed and reduced or even avoided in other regions to preserve details. [5]

2.11.2.2 Multi Scale Methods

Several multi scale methods based on wavelet and pyramid have been proposed for speckle reduction in ultrasound imaging.

2.11.2.2.1 Wavelet based speckle reduction methods

The wavelet based speckle reduction method usually include (1) logarithmic transformation (2) wavelet transformation (3) modification of noisy coefficient using shrinkage function (4) invert wavelet transform and (5) exponential transformation. This method can be classified into three groups:

- Thresholding methods** - The wavelet coefficients smaller than the predefined threshold are

regarded as contributed by noise and then removed. The thresholding techniques have difficulty in determining an appropriate threshold.

- Bayesian estimation methods** – This Method approximates the noise free signal based on the distribution model of noise free signal and that of noise . Thus, reasonable distribution models are crucial to the successful application of these techniques to medical ultrasound imaging.

- Coefficients correlation methods** - This is an undecimated or over complete wavelet domain denoising method which utilizes the correlation of useful wavelet coefficients across scales .

However this method does not rely on the exact prior knowledge of the noise distribution and this method is more flexible and robust compared to other wavelet based methods. [5]

2.11.2.2.2 Pyramid based speckle methods

Pyramid transform has also been used for reducing speckle. Approximation and interpolation filters in pyramid transform have low pass properties so that pyramid transform does not require quadrature mirror filters unlike sub band decomposition in wavelet transform.

- A ratio laplacian pyramid was introduced by considering the multiplicative nature of speckle .

This method extended the conventional Kaun filter to multi scale domain by processing the inter scale layers of the ratio laplacian pyramid. But this

method differs from the need to estimate the noise variance in each inter scale layers. [5]

2.12 Speckle models

Although the existing despeckling filters are termed as edge and feature preserving filters some major limitation exists:

1. The filters are sensitive to the noise components .
2. Noise attenuation is not sufficient especially in the smooth and background areas.
3. The existing filters do not enhance edges but they only inhibit smoothing near edges Thus, effective despeckling requires an accurate statistical model of ultrasound signals.

A generalized model of the speckle imaging can be written as:

$$\mathbf{g} = \mathbf{fn} + \mathbf{m} \quad (2.3)$$

Let g denote the observed signal, m, n the multiplicative and additive components of noise respectively introduced by the acquisition process and f the original signal without noise.

Generally the effect of additive noise is very small compared to multiplicative noise, so the simplified noise model:

$$\mathbf{g} = \mathbf{fn} \quad (2.4)$$

Thus the logarithmic compression transforms the model in (2) into the classical signal in additive noise form as:

$$\mathbf{Log} \mathbf{g} = \mathbf{log} \mathbf{f} + \mathbf{log} \mathbf{m} \quad (2.5)$$

The statistics of speckle noise can be categorized into different classes according to number of scatterers per resolution cell called scattered number density (SND). In the case of many fine randomly distributed scatterers per resolution cell (>10) the speckle can be modeled by a Rayleigh distribution with a constant SNR of 1.92. When the scattered densities are smaller a generalized version of Rayleigh distribution called the K-distribution can be used. For high SNR the Rician model can be used, and also for lower SNR the speckle can be modeled using Homodyne K-distribution. [5]

2.13 Despeckling filter

In order to be able to derive an efficient despeckle filter, a speckle noise model is needed. The speckle noise model may be approximated as multiplicative, if the envelope signal received at the output of the beam former of the ultrasound imaging system is captured before logarithmic compression. Logarithmic compression is applied to the envelope-detected echo signal in order to fit it in the display range. Speckle filtering consists of moving a kernel over each pixel in the image and applying a mathematical calculation using the pixel values under the kernel and replacing the central pixel with the calculated value. The kernel is moved along the image one pixel at a time until the entire image has been covered. By applying the filter a smoothing effect is achieved and the visual appearance of the speckle is reduced. An appropriate method for speckle reduction is one which enhances the signal-to noise ratio while conserving the edges and lines in the image. Filtering techniques are used as a preface action before segmentation and classification. In literature many techniques have been studied for speckle noise reduction. [6]

2.13.1 Homogeneous Mask Area Filtering

The (lsminsc) Minimum speckle index homogeneous mask despeckle filter is a 2-D filter operating in a 5×5 pixel neighborhood by searching for the most homogeneous neighborhood area around each pixel, using a 3×3 subset window. The middle pixel of the 5×5 neighborhoods is substituted with the average gray level of the 3×3 mask with the smallest speckle index, where C represents the variance over mean of the 3×3 window. [6]

2.13.2 Median Filtering

The filter (median) and (hybrid median) is a simple nonlinear operator that replaces the middle pixel in the window with the median-value of its neighbors. The moving window for the median filter was 7×7 , it is particularly effective to remove pulse or spike noises. The main problem of the median filter is its high computational cost for sorting N pixels. [6]

2.13.3 Linear Scaling Filter

1. The (ca) Linear scaling of the gray-level despeckle filter, this filter despeckle the image through linear scaling of the gray-level values . In a window of 5×5 pixels, compute the mean of all pixels whose difference in the gray level with the intensity (the middle pixel in the moving window) is lower than or equal to a given threshold .
2. The (lecasort) Linear scaling and sorting despeckle filter takes k points of a pixel neighborhood, which are closest to the gray level of the image at point (the middle point in the moving window) , including It then assigns the mean value of these points to the pixel. [6]

2.13.4 Geometric Filtering

The concept of the geometric filtering is that speckle appears in the image as narrow walls and valleys. The geometric filter, through iterative repetition, gradually tears down the narrow walls (bright edges) and fills up the narrow valleys (dark edges), thus smearing the weak edges that need to be preserved, The(gf4d) Geometric despeckle filter uses a nonlinear noise reduction technique. It compares the intensity of the central pixel in a 3×3 neighborhood with those of its eight neighbors and, based upon the neighborhood pixel intensities, it increments or decrements the intensity of the central pixel such that it becomes more representative of its surrounding. [6]

2.13.5 Anisotropic Diffusion Filtering

Perona and Malik (ad), it depend on function, called the diffusion coefficient ,which is a monotonically decreasing function of the gradient magnitude ,yields in traregion smoothing and not inter region smoothing by impeding the diffusion at image edges. It increases smoothing parallel to the edge and stops smoothing perpendicular to the edge, as the highest gradient values are perpendicular to the edge and dilated across edges. [6]

2.13.6 Wavelet Filtering

The wavelet techniques are widely used in the image processing, such as the image compression, image de-noising. It has been shown that its performance of image processing is better than the methods based on other linear transformation. The wavelet de-noising method decomposes the image into the waveletbasis and shrinks the wavelet coefficients in order to despeckle the image. From the noisy image, global soft threshold coefficients are calculated for every decomposition level . After the thresholding, the imageis reconstructed by inverse wavelet transforming and the despeckled image is derived. Speckle reduction filtering in the wavelet domain (waveltc) Wavelet despeckle filter, used in this study, is based on

the idea of the DaubechiesSymlet wavelet and on soft-thresholding denoising.[6]

2.13.7 Total variation denoising

Total variation denoising (TVD) is an approach for noise reduction developed so as to preserve sharp edges in the underlying signal. Unlike a conventional low-pass filter, TV denoising is defined in terms of an optimization problem. The output of the TV denoising 'filter' is obtained by minimizing a particular cost function.

$$U = f - P_{GA}(f) \quad (2.6)$$

Where f is the noisy image, U is the image we want to restore from $f - P_{GA}(f)$ is the orthogonal projection of f on GA and the space G is proposed by Meyer for modeling oscillating patterns . [14]

2.14 Limitation of despeckle filtering techniques

Despeckling is always a tradeoff between noise suppression and loss of information, which is something that experts are very concerned about. It is, therefore, desirable to keep as much important information as possible. The majority of speckle reduction techniques have certain limitations that can be briefly summarized as follows.

They are sensitive to the size and the shape of the window. The use of different window sizes greatly affects the quality of the processed images. If the window is too large, over smoothing will occur, subtle details of the image will be lost in the filtering process, and edges will be blurred.

On the other hand, a small window will decrease the smoothing capability of the filter and will not reduce the speckle noise, thus making the filter not effective. In homogenous areas, the larger the window size, the more coefficient the filter in reducing the speckle noise. In heterogeneous areas, the smaller the window size, the more it is possible to keep subtle image details unchanged. Our experiments showed that a [7 X7] window size is a fairly good choice. Some of the despeckle methods based on window approaches require thresholds to be used in the filtering process, which have to be empirically estimated. There are a number of thresholds introduced in

the literature, which include gradient thresholding , soft or hard thresholds , nonlinear thresholds , and wavelet thresholds . The inappropriate choice of a threshold may lead to average filtering and noisy boundaries, thus leaving the sharp features unfiltered. Most of the existing despeckled filters do not enhance the edges, but they only inhibit smoothing near the edges. When an edge is contained in the filtering window, the coefficient of variation will be high, and smoothing will be inhibited. Therefore, speckle in the neighborhood of an edge will remain after filtering. They are not directional in the sense that in the presence of an edge, all smoothing is precluded. Instead of inhibiting smoothing in directions perpendicular to the edge, smoothing in directions parallel to the edge is allowed. Different evaluation criteria for evaluating the performance of despeckled filtering are used by different studies. Although most of the studies use quantitative criteria like the MSE and the speckle index (C), there are additional quantitative criteria like texture analysis and classification, image quality evaluation metrics, and visual assessment by experts that could be investigated. [9]

2.15 Image quality evaluation metrics

To quantify the performance improvements of the speckle reduction method various measures may be used. The commonly preferred measures root mean squared error (RMSE) ,structural similarity index(SSIN), signal to noise ratio (SNR) ,peak signal to noise ratio (PSNR). [6]

The root mean square error(RMSE) :

This measures the quality change between the original and processed image in an $M \times N$ window.

The root mean square error (RMSE), which is the square root of the squared error averaged over an $M \times N$ window : [6]

$$\text{RMSE} = \sqrt{\frac{1}{MN} \sum_{i=1}^M \sum_{j=1}^N (g_{i,j} - f_{i,j})^2} \quad (2.7)$$

The structural similarity index (SSIN) :

$$\text{SSIN} = \frac{(2\bar{g}\bar{f}+c_1)(2\sigma_{gf}+c_2)}{(\bar{g}^2+\bar{f}^2+c_1)(\sigma_g^2+\sigma_f^2+c_2)}, -1 < \text{SSIN} < 1 \quad (2.8)$$

Where $c1 = 0.01dr$ and $c2 = 0.03dr$, with $dr = 255$ representing the dynamic range of the ultrasound images. The range of values for the SSIM lies between -1 , for a bad and 1 for a good similarity between the original and despeckled images, respectively. It is computed, for a sliding window of size 8×8 without overlapping. [6]

The signal to noise ratio(SNR) given by:

$$\text{SNR} = 10 \log_{10} \frac{\sum_{i=1}^M \sum_{j=1}^N (g_{i,j}^2 + f_{i,j}^2)}{\sum_{i=1}^M \sum_{j=1}^N (g_{i,j} - f_{i,j})^2} \quad (2.9)$$

The peak signal to noise ratio(PSNR) given by:

$$\text{PSNR} = -10 \log_{10} \frac{\text{MSN}}{g_{\max}^2} \quad (2.10)$$

Where g_{\max} is the maximum intensity in the unfiltered image. The PSNR is higher for a better-transformed image and lower for a poorly transformed image. It measures image fidelity, which is how closely the despeckled image resembles the original image. [6]

2.16 Edge detection

Edge detection is defined as a process to identify the sharp discontinuities in an image. The discontinuities are often known as abrupt changes in pixel intensity or the pixels that characterize the boundaries of objects in an image. The edge detected contributes in many applications such as image segmentation , enhancement , compression and etc . The edge detection in digital image processing is always implemented by convolving the image with a 2D filter operator. The 2D filter is designed to be of high sensitivity towards large gradients in the image and return null values on pixels in homogenous region of image. Edge detection is a significant issue in image processing and pattern recognition. It is due to its ability to give the outline of an object, to supply information of the boundary between an object and background, to indicate overlapping objects, to calculate the basic properties of the object like area and shape and to classify and identify essential information in image. The desired effect of any edge detection operation is giving no response to non-edge pixels and giving only one response to a

single edge .Multitude algorithms of edge detection have been proposed . Among the common edge detection methods are Sobel method ,canny, Roberts , Prewitt and Laplacian method , Rosenfeld and Thurston and Marr-Hildreth. These methods detect edges by utilizing masks to perform the convolution on the digital image according to the sudden change of gray level pixel intensity. [11]

2.16.1 Canny operator

Canny operator uses Gaussian convolution technique first to smooth the image, and then measured the gradient properties in the image by a set of Robert’s cross convolution masks. It uses a filter based on the first derivative of a Gaussian, to for smoothing of image followed by the derivative of the gaussian, which is in one dimension since it is susceptible to noise present on raw unprocessed image data, so to begin with, the raw image is convolved with a Gaussian filter. The result is a slightly blurred version of the original which is not affected by a single noisy pixel to any significant degree. [10]

2.16.2 Sobel operator

Sobel operator is used in image processing techniques particularly in edge detection. The sobel operator is based on convolving the image with a small, separable, and integer valued filter in horizontal and vertical and is therefore relatively inexpensive in terms of computations. The Sobel operator uses a mask to performs a 2-D spatial gradient measurement on an image and so emphasizes regions of high spatial frequency that correspond to edges. Typically it is used to find the approximate absolute gradient magnitude at each point in an input grayscale image. [10]

1-	2	1-
0	0	0
1	2	1

1-	0	1
2-	0	2
1-	0	1

2.16.3 Prewitt operator

Prewitt operator edge detection masks are the one of the oldest and best understood methods of detecting edges in images. Basically, there are two masks, one for detecting image derivatives in X and one for detecting image derivative in Y. To find edges, a user convolves an image with both masks, producing two derivative images (dx and dy). The strength of the edge at given location is then the square root of the sum of the squares of these two derivatives. The set of kernels is limited to 8 possible orientations; however experience shows that most direct orientation estimates are not much more accurate. On the other hand, the set of kernels needs 8 convolutions for each pixel, whereas the set of kernel in gradient method needs only 2, one kernel being sensitive to Mathematical morphology is used to study geometric structure of images .The basic idea above is to apply a structuring element to detect an image, to see whether the structuring element can be filled in the internal of the image well and to validate the validity of the method. The mathematical foundation of morphology and all languages used is set theory which is composed of a group of algebraic calculation. The four basic operations are dilation, erosion, opening and closing. These basic operations are used to process binary image firstly, the basic theory is binary morphology. The binary morphology has natural extensions to Gray-scale morphology. The image which will be processed by mathematical morphology theory must be changed into set and represented as matrix. [10]

1-	1-	1-
0	0	0
1	1	1

1-	0	1
1-	0	1
1-	0	1

2.16.4 Robert operator

The Robert Cross operator performs a simple and quick 2-D spatial gradient measurement on an image. The operator consists of a pair of 2 x2 convolution kernel. These kernels are designed to respond maximally to edges running at 45o to the pixel grid one kernel for each of the two

perpendicular orientations. The kernels can be applied separately to the input image to produce separate measurement of the gradient component in each orientation these can then be combined together to find the absolute magnitude of the gradient at each point and orientation of the gradient is represented by: [12]

0	+1
-1	0

+1	0
0	1

$$\text{localization} = \frac{1}{\sqrt{E[X_0^2]}} \tag{2.11}$$

$$= \frac{\int_{-w}^w g'(-x)f'(x)dx}{\sqrt{\int_{-w}^w f''(x)dx}} \tag{2.12}$$

2.16.5 laplacian operator

The Laplacian method searches for zero crossing in the second derivative of the image to find edges .Various detection method have been developed over the years, these techniques can be classified into pixel-level and sub pixel level edge detection. Early detection method employed local operators to approximately compute the first derivative of grey level gradient of an image in spatial domain. The location of local maximum of the first derivative and considered to be edge points Prewitt and Sobel operators are examples of gradient based edge detections . Marr and Hildreth proposed the Laplacian of Gaussian (LOG) for edge detection which uses Gaussian function for image smoothing, then calculates second derivative. The zero crossing point is considered to be edge points. Canny operator gives the information of both intensity and direction. All method mentioned above are pixel-level edge detection capable of detecting edge fast but low precision. One of the earliest techniques for sub pixel edge detection was proposed by Hueckel. Hke determined edge parameters by fitting image data to a Hilbertspace of

nine points and then the point is declared as an edge point, if the computed edge parameter values for that point are sufficient close to the ideal edge model. [13]

The laplacian $L(x,y)$ of an image with pixel intensity values $I(x,y)$ given by:

$$L(x,y) = \frac{\partial^2 I}{\partial x^2} + \frac{\partial^2 I}{\partial y^2} \quad (2.13)$$

The 2-D LOG function centered on zero and with gaussian stander deviation has the form:

$$\text{LOG}(x,y) = \frac{1}{\pi^4} \left[1 - \frac{x^2+y^2}{2\sigma^2} \right] e^{-\frac{x^2+y^2}{2\sigma^2}} \quad (2.14)$$

1	1	1
1	8	1
1	1	1

1-	2	2-
2	4-	2
1-	2	1-

Literature review

S.Kalaivani Narayanan and R.S.D.Wahidabanu, A View on Despeckling in Ultrasound Imaging (2009) in this paper developing an efficient and robust denoising method for ultrasound images one has to take into account number of factors. The choice of despeckling filter and speckle model plays an important role in the design of despeckling methods and it differs from application to application. Most commonly preferred models and filters were discussed with its merits and demerits.

Ehsan Nadernejad, Mohammad Reza Karami , Sara Sharifzadeh and Mostafa Heidari , Despeckle Filtering in Medical Ultrasound Imaging (2009), In this paper, we implemented Wiener filter, anisotropic diffusion filter, kdistribution based adaptive filter and wavelet filter to de speckle in medical ultrasound images.

Arpit singhal , mandeep singh ,speckle noise removal and edge detection using mathematical morphology(2011)In this paper a novel mathematical morphology algorithm is proposed which is use to remove speckle noise from the image and find the edge more efficiently then the previously used edge detector like sobel ,prewitt and canny and filters used to remove speckle noise like LEE and SARD.

Milin dkumar V. Sarode and Prashant R. Deshmukh (2011) Reduction of Speckle Noise and Image Enhancement of Images Using Filtering Technique, We introduced a Speckle noise reduction model for Ultrasound Sound images as well as Synthetic Aperture Radar (SAR) imagery. Both models preserve the appearances of structured regions. In case of Ultrasound Images, Texture and organ surfaces have been enhanced. The performance of the algorithm has been tested using visual performance measures. Many of the methods are failure to remove speckle noise present in the Ultrasound images, since the information about the variance of the noise may not be able to identify by the methods. Introduced model automatically collect the information about the noise variance. Performance of the Speckle noise reduction model for Synthetic Aperture Radar (SAR) imagery is well as compared to other filters. Histogram results shows very closed equivalency in between SAR original images and SAR denoised i.e. enhanced images.

HUM YAN CHAI , LAI KHIN WEE , EKO SUPRIYANTO , Edge Detection in Ultrasound Images Using Speckle Reducing Anisotropic Diffusion in Canny Edge Detector Framework , This paper presented an improved Canny edge detector by incorporating it with Speckle reducing anisotropic diffusion method in eight directions which can adapt to ultrasonic local speckle statistic. Experimental results on ultrasound phantom shows that the proposed method can preserve edges and small structures while removing speckle noise effectively at a wide range of threshold and standard deviation. Thus, it has the potential to enhance the diagnostic ultrasound imaging and to improve automated segmentation and edge detection technique. Future efforts should be focus on the thresholding step in Canny edge detection in order to make it become more adaptive to the noisy image.

Banazier Ahmed Ibrahim and Yasser M. Kadah, Comparative Evaluation of Despeckle Filtering Techniques In Medical Ultrasound Imaging , The use of filter in Digital Image Processing improves the image to a great extent. Mainly in the case of presence of Speckle noise, filtering is very much required in order to improve the diagnostic examination and also to improve the efficiency of post processing techniques like segmentation.

Despeckle filtering is an important operation in the enhancement of ultrasonic imaging. In this study it was shown that simple filters based on linear scaling filter (*lecasort*) , geometric filtering (*gf4d*) ,diffusion filter (*srad*) , local statistics (*lsmv*) and nonlinear filtering (*hybrid median*)could be used successfully for the processing of these images. Thus, while developing an efficient and robust denoising method for ultrasound images one has to take into account number of factors. The choice of despeckling filter and speckle model plays an important role in the design of despeckling methods and it differs from application to application. Most commonly preferred models and filters were discussed with its merits and demerits in this paper. Initial findings show promising results from several filters, different clinical images are required to evaluate the performance of the filters. Other filtering methods may also be studied to compare with these filters. Finally we can say the *Srad* , *gf4d* and *lecasort* filters are noted to be effective in suppressing speckle noise than other filtering techniques, both objectively and subjectively , not only remove speckle but also preserve the details of the image, and preserves the edge properties and Geometric filtering (*gf4d*) is the best one . Initial findings show promising results; however, further work is required to evaluate the performance of the

suggested despeckle filters at a larger scale as well as their impact in clinical practice, and to carry out another a comparative evaluation of despeckle filtering based on texture analysis, distance measures , and KNN classifier . In addition, the usefulness of the proposed despeckle filters in portable ultrasound systems and in wireless telemedicine systems still has to be investigated.

Ferdous hossain ,mina asaduzzaman , mohammad abu yousuf and Md Armanur rahman dynamic thresholding based adaptive canny edge detection in this paper ,a method for adaptive canny edge detection algorithm is proposed . adaptive canny algorithm is used to increase accuracy of out put object, in this paper an effective method for edge detection via daynamic thresholding of adaptive canny algorithms.

Sophia and J.Maria divyalnfanta M.Phil scholar, Various edge detection methods are analysed .The methods are applied with the algorithms .no specific texture or shape is specified . it can be shown clearly that the Sobel ,perwitt ,and Robert provide low quality edge maps relative to others.

Jaspreet Kaur and Anand Sharma Study many edge detection techniques are discussed like Sobel operator technique, Roberts cross techniques ,prewitt technique and canny technique ,etc. these edge detection techniques are selected based on the same environmental conditions .Gradient based operators are very sensitive to noise.

Shaveta malik and tapas kumar (2016) comparative Analysis of Edge Detection between Gray Scale and Color image vector-valued techniques used for the detection edges in color images. color edge operators are able to detect more edge than gray – level edge operator.

Pinaki patim acharjya , Ritaban Das , Dibyendu Ghoshal a study and comparative analysis of various gradient based image edge detection techniques is presented .in image processing and image analysis edge detection is one of the most common operations .Edges form the outline of an object and also it is the boundary between an object and the background. Detection accurate edges are very important for analyzing the basic properties associated with an image such as area , perimeter and shape . the software tool that has been used is MATLAB7.

4.1 Materials and methodology:

This chapter explain the materials and steps of hybrid technique which is improvement of the disadvantage of despeckle filtering and edge detection in using to enhance and better for preserving the image texture.

Proposed method sobel edge detection hybrid with sort filter (SO_SORT):

Algorithm:

Methodology:

Step1:Load image: Three different medical ultrasound imaging datasets were used in this research (liver , kidney and fetal).

- Step2:
- Adding speckle noise ;we added speckle noise (0.5 and 0.05) to original image.
- Filtering; we use 9 speckle reduction filters (local statistics, homogenous , mask area median filtering, hyper median filtering , linear Scaling filter, geometric filtering, speckle reduction anisotropic diffusion filtering, Total variation filtering , and wavelet filtering).

Step3:Compute IMQs: Differences between the original and despeckled images were evaluated using image quality evaluation metrics(root mean square error (RMSE), , peak signal to noise ratio(PSNR), signal to noise ratio(SNR), Structural similarity index(SSIM)) and find the best filter.

- Histogram : we show histogram for original and despeckle images to find the gray level of image and best filter.
- Step4: Post processing (edge detection and compute IMQs) : from preprocessing step we find the best despeckle filtering; then by using original and despeckle image we applied five edge detection operators (canny- sobel - prewitt –roberts - and laplacian of gaussian) and compute IMQs to evaluated the result and chose best edge operator.

- Step5: We found the final result by Applying three best despeckle filter (speckle reduction anisotropic diffusion filtering , Linear Scaling(NeighborHood Averaging)Filtering and Linear Scaling filtering)on the image with best edge detection(SOBEL) and then find the best of them corresponding to IMQs evaluation ; that denoise image and preserving the information .

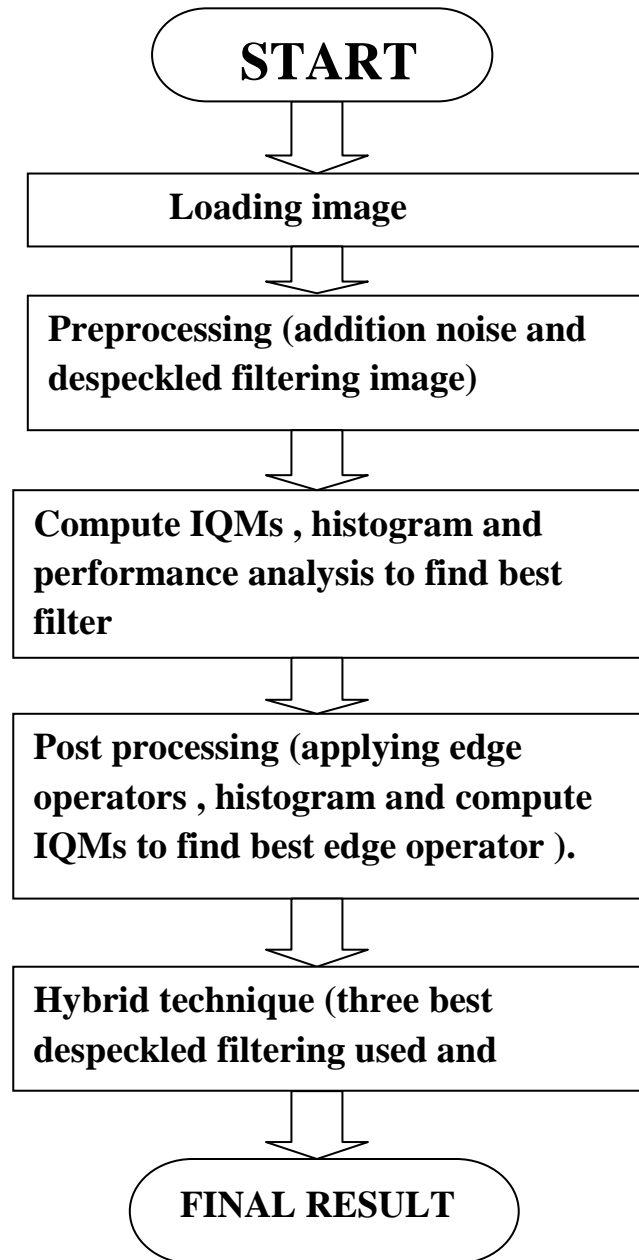


FIGURE4.1: flow chart of proposed method.

5.1 Experimental result:

speckle reduction anisotropic diffusion filtering , Linear Scaling(Neighborhood Averaging)Filtering and Linear Scaling filtering)on the image with best edge detection(SOBEL) hybrid technique has been implemented in the MATLAB environment. Various US B-scan images from the, and IBE Tech (Giza.Egypt) database of ultrasound image including liver and fetal , ultrasound scanmalaysia.com including kidney. . And artificially corrupted by speckle noise (multiplication noise) with variance $\sigma_n = 0.05$ and 0.5 using the MATLAB command "imnoise (image, „speckle“, 0.05 or 0.5)".

To estimate the performance of the hybrid technique. Nine standard filters namely: linear scaling gray level filter(DsFca),geometric despeckle filter(DsFg4d),median filter(Dsfmedian),hyper median filter(Dsfhypermedian),homogenous mask area (Dsflminsc) speckle reducing anisotropic diffusion(srad),wavelet filter (Dsfwavelet)and total variation denoising (TVD), Linear Scaling(Neighborhood Averaging)Filtering(Dsflcasort) ;edge detection sobel ,Robert ,prewitt , lablacian of gaussian and canny have been implemented in the same US images with both variance value. To quantify the performance improvements of the speckle reduction method and preserve feature various measures may be used. The commonly preferred measures are root mean squared error (RMSE), signal to noise ratio (SNR), peak signal to noise ratio(PSNR) and structural similarity index(SSIM), which have been calculated from the denoised US images and are found in the literatures. The PSNR and SNR is higher for a better-transformed image and lower for a poorly transformed image, on the contrary in RMSE. Whilst the range of values for the SSIM lies between -1, for bad and 1 for good similarity between the original and despeckled images.

In this chapter the differences between the original, and the despeckled images were evaluated using image quality evaluation metrics (IQMs). The following measures, which are easy to compute and have clear physical meaning.

Result of preprocessing

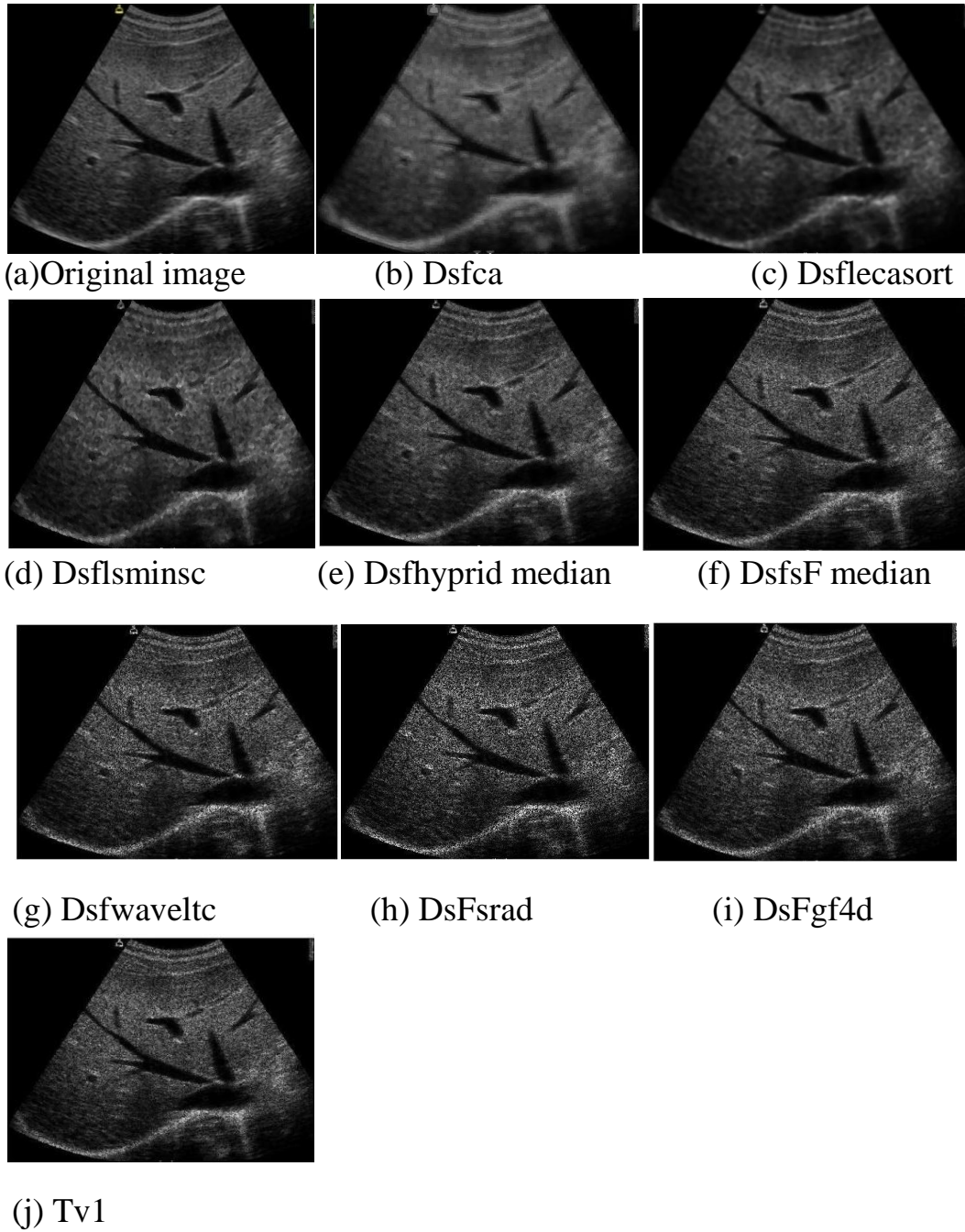


FIGURE 5.1: Results of liver despeckled by various filter on multiplication noise ($\sigma_n=0.5$).

Table5.1: Image quality evaluation metrics computed for the Liver ($\sigma = 0.5$) at statistical measurement of RMSE,PSNR, SNR and SSIM for different filter types.

Types of filter	Images quality metrics			
	RMSE	PSNR	SNR	SSIM
Dsfca	14.7638	24.7809	18.7672	0.4557
Dsflecasort	17.8408	23.1365	18.7072	0.6882
Dsflsminsc	24.8691	20.2516	18.4962	0.6351
DsFsrاد	15.8238	24.1786	19.0140	0.6685
Dsfsmedian	36.0904	18.5679	17.0170	0.3713
Dsfhypridmedian	22.3629	21.1742	18.5341	0.6237
Dsfwaveltc	38.8954	18.8765	16.3668	0.4060
DsFgf4	37.8405	21.6530	16.6075	0.4007
Tv	18.4901	22.8260	18.2126	0.1183

Bold number indicates the best values.

* signal-to-noise ratio (SNR), peak-to-noise ratio (PSNR), structural similarity index(SSIM) and root mean square error(RMSE).

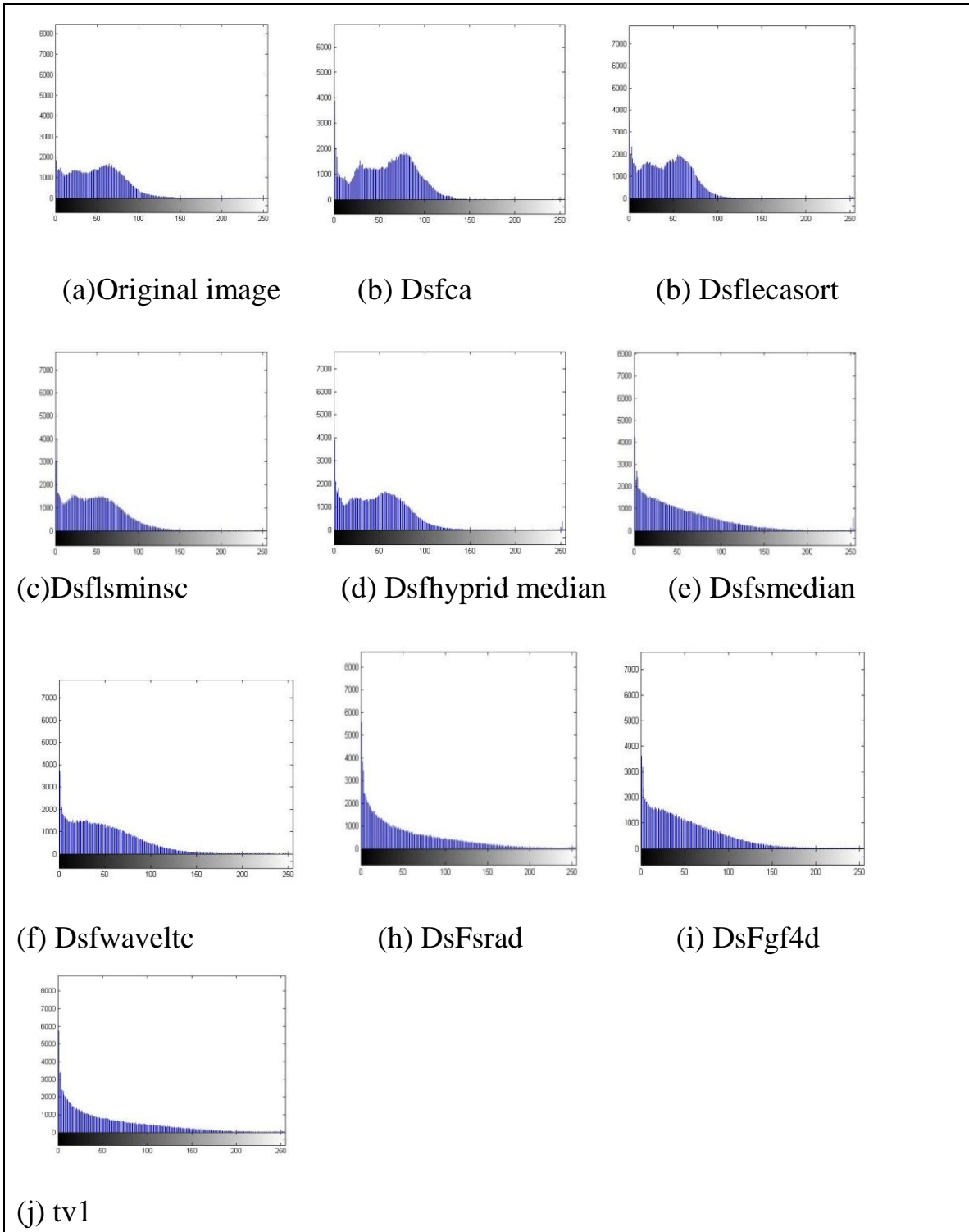


FIGURE 5.2: Histogram result of liver despeckled by various filter on multi active noise(noise =0.5).

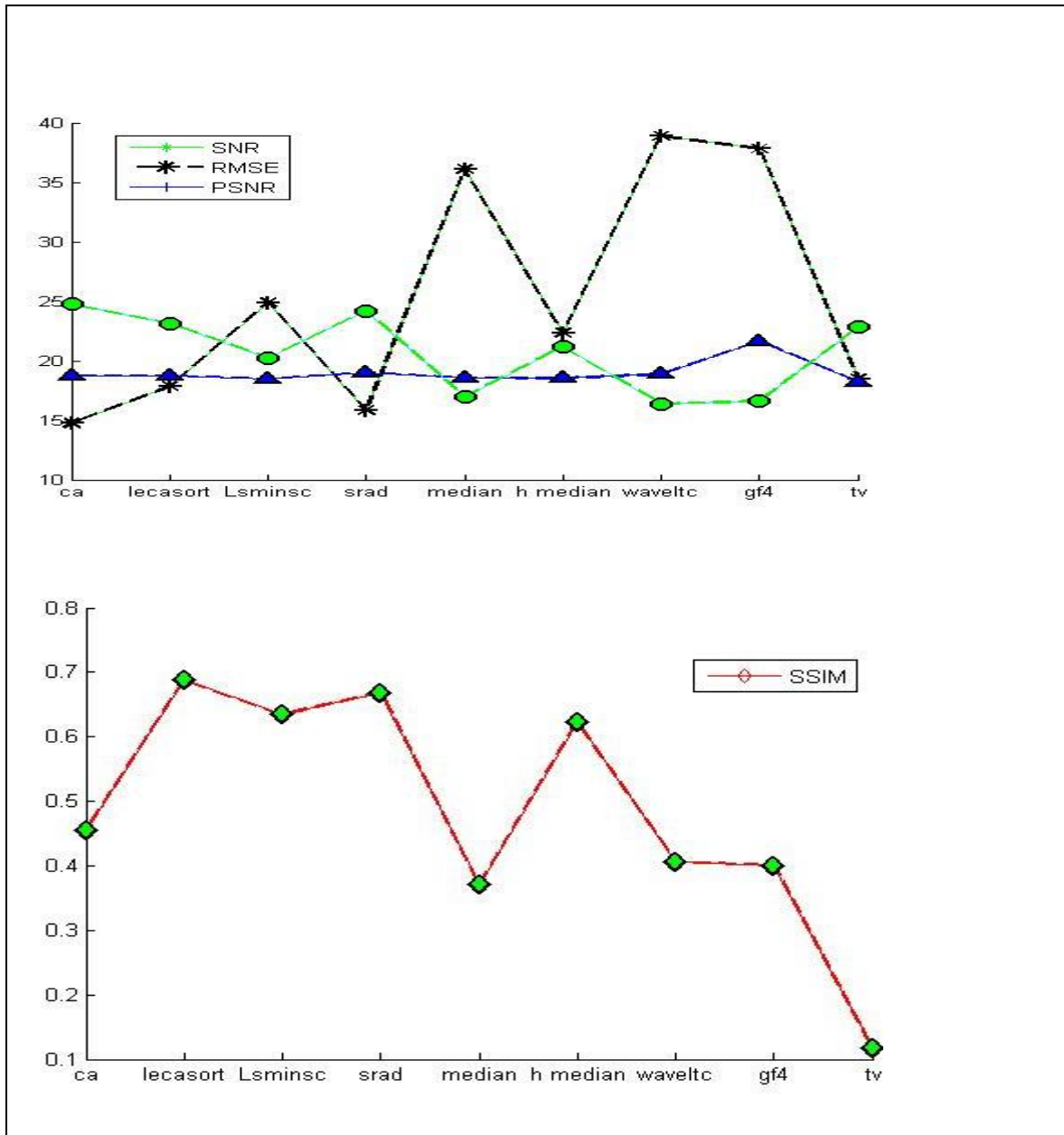
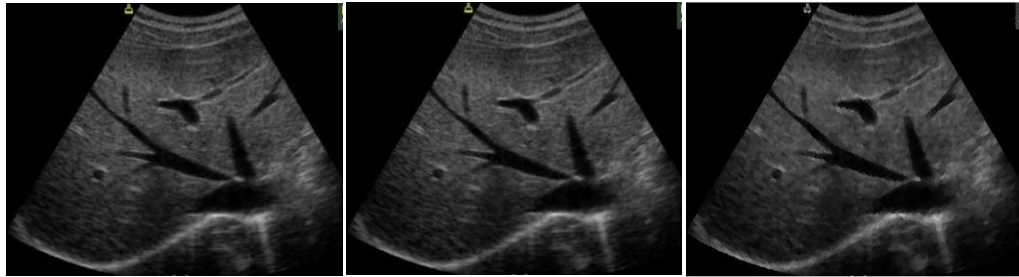


FIGURE 5.3: Performance analysis graph to image quality evaluation metric for liver image (noise $\sigma_n = 0.5$).



(a)Original image

(b) Dsfca

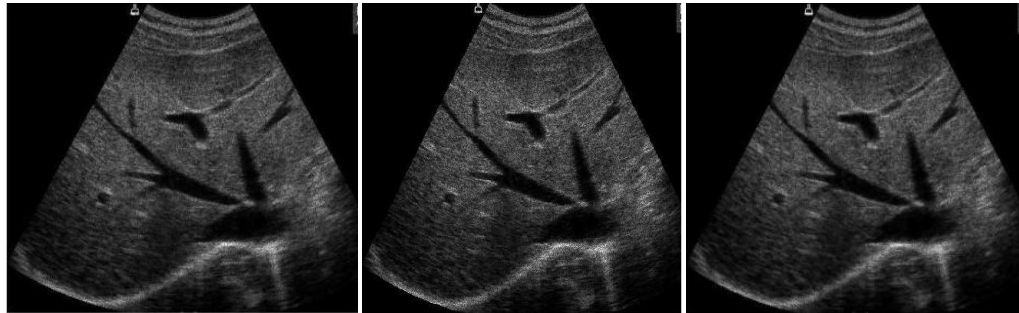
(c) Dsflecasort



(d) DsFflsminsc

(f) Dsfhybrid median

(g) Dsfwaveltc



(h)DsFsrad

(i) DsFgf4d

(j) DsFgf4d



(j) TV

FIGURE 5.4: Results of liver despeckled by various filter on multiplication noise ($\sigma_n=0.05$).

Table5.2: Image quality evaluation metrics computed for the Liver ($\sigma=0.05$) at statistical measurement of **RMSE**, **SNR**, **PSNR** and **SSIM** for different filter types.

Types of filter	Images quality metrics			
	RMSE	PSNR	SNR	SSIM
Dsfca	15.7009	24.2463	18.5557	0.6975
Dsflecasort	24.6244	20.3375	18.4600	0.6671
Dsflsminsc	19.7783	22.2410	18.4990	0.7312
DsFsrاد	19.0824	22.5522	18.5470	0.7389
Dsfsmedian	24.8942	20.2428	18.6278	0.6159
Dsfhybridmedian	19.91227	22.1822	18.4996	0.7667
Dsfwaveltc	20.3876	21.9775	18.5280	0.6580
DsFgf4	24.1301	20.5136	18.6174	0.5743
Tv	20.0713	22.1133	21.6100	0.7160

Bold number indicates the best values.

* signal-to-noise ratio (SNR), peak-to-noise ratio (PSNR), structural similarity index(SSIM) and root mean square error(RMSE).

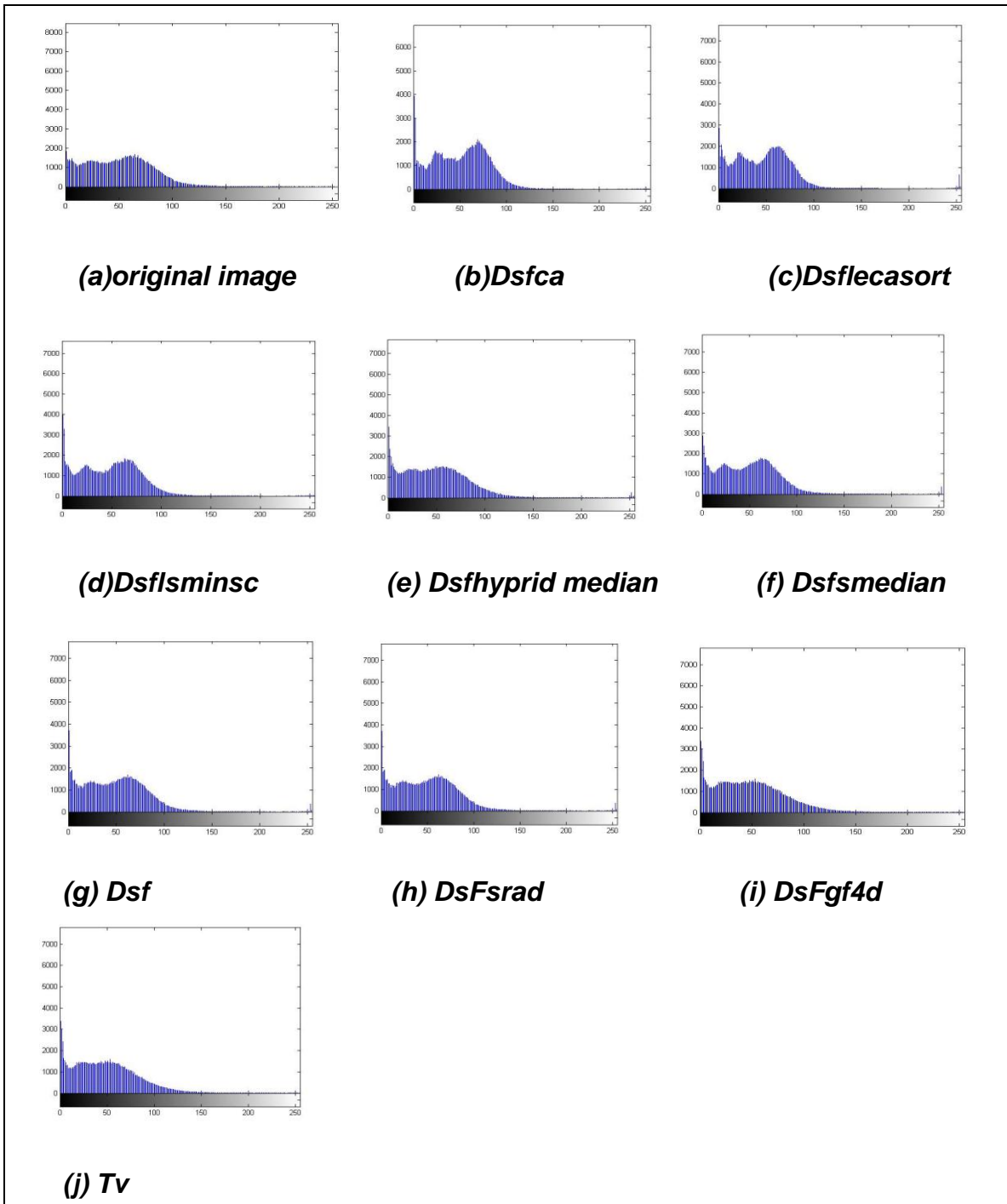


FIGURE 5.5: Histogram result of liver despeckled by various filter on multiplication noise(noise =0.05).

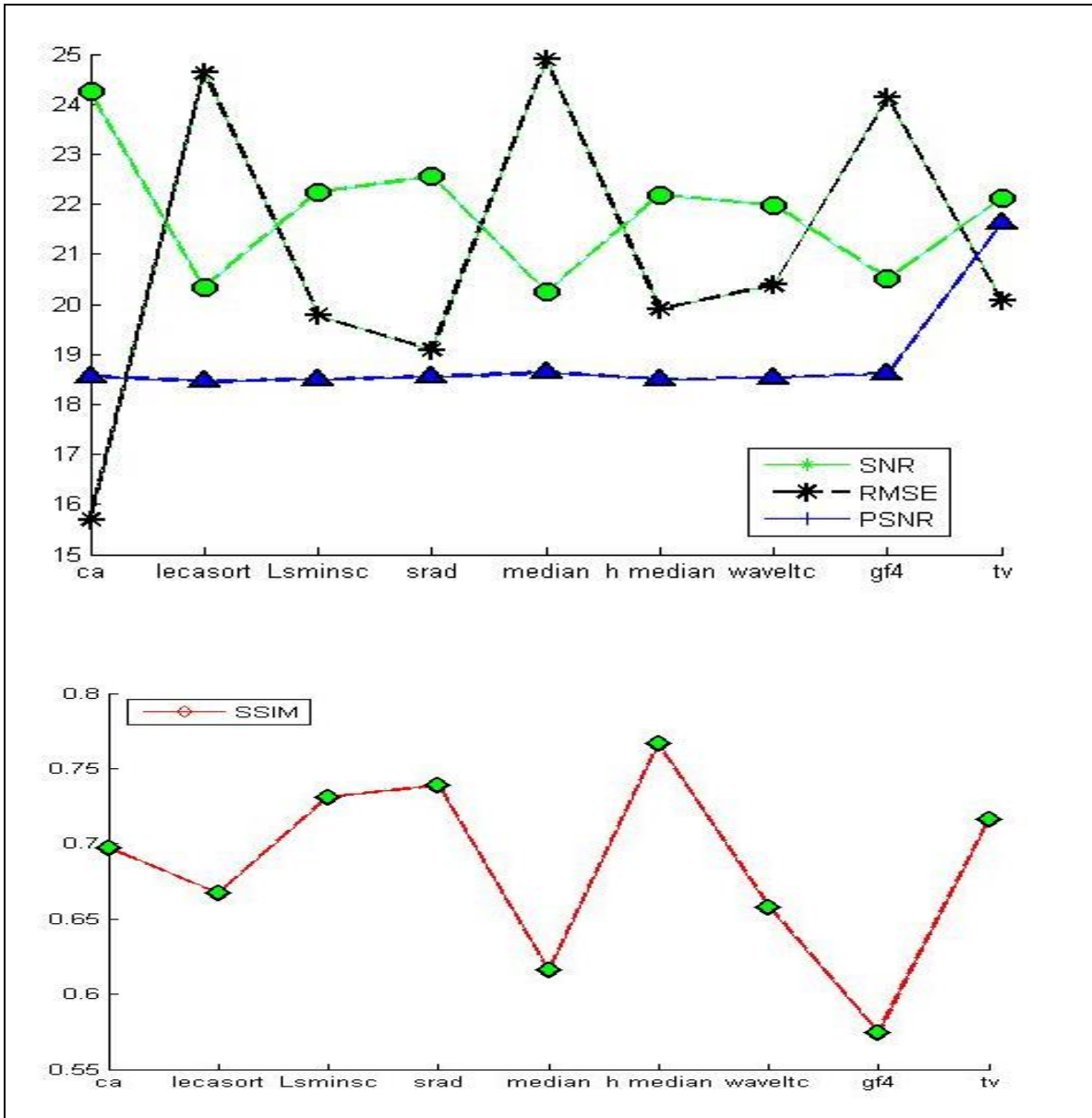


FIGURE 5.6:Performance analysis graph to image quality evaluation metric for liver image (noise $\sigma_n = 0.05$).

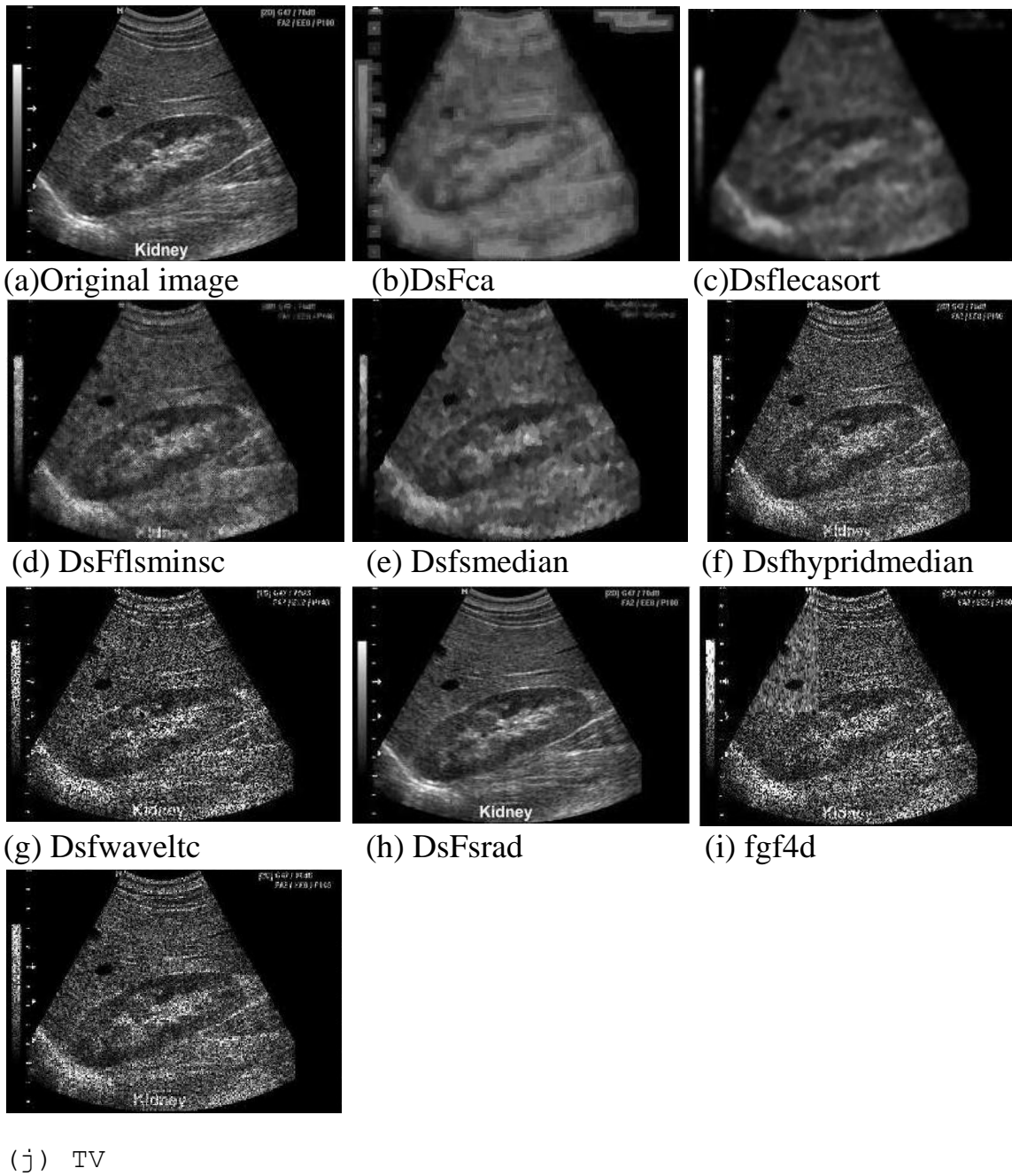


FIGURE 5.7: Results of kidney despeckled by various filter on multiplication noise ($\sigma_n=0.5$).

Table5.3: Image quality evaluation metrics computed for the kidney ($\sigma_n=0.5$) at statistical measurement of RMSE,PSNR, SNR and SSIM for different filter types.

Types of filter	Images quality metrics			
	RMSE	PSNR	SNR	SSIM
Dsfca	27.5543	19.3610	19.8643	0.4761
Dsflecasort	33.9543	17.5469	19.2485	0.5514
Dsflsminsc	20.6441	21.8689	19.4210	0.6048
DsFsrاد	28.2039	19.1586	20.0567	0.5569
Dsfsmedian	40.0254	16.1181	19.8458	0.4421
Dsfhybridmedian	34.3591	17.4440	19.6011	0.5142
Dsfwaveltc	52.5148	13.7592	19.7393	0.3770
DsFgf4	48.2652	14.4921	20.1124	0.4172
Tv	69.0909	16.4754	22.7977	0.1137

Bold number indicates the best values.

* Signal -to- noise ratio (SNR), peak-to-noise ratio (PSNR), structural similarity index(SSIM) and root mean square error(RMSE).

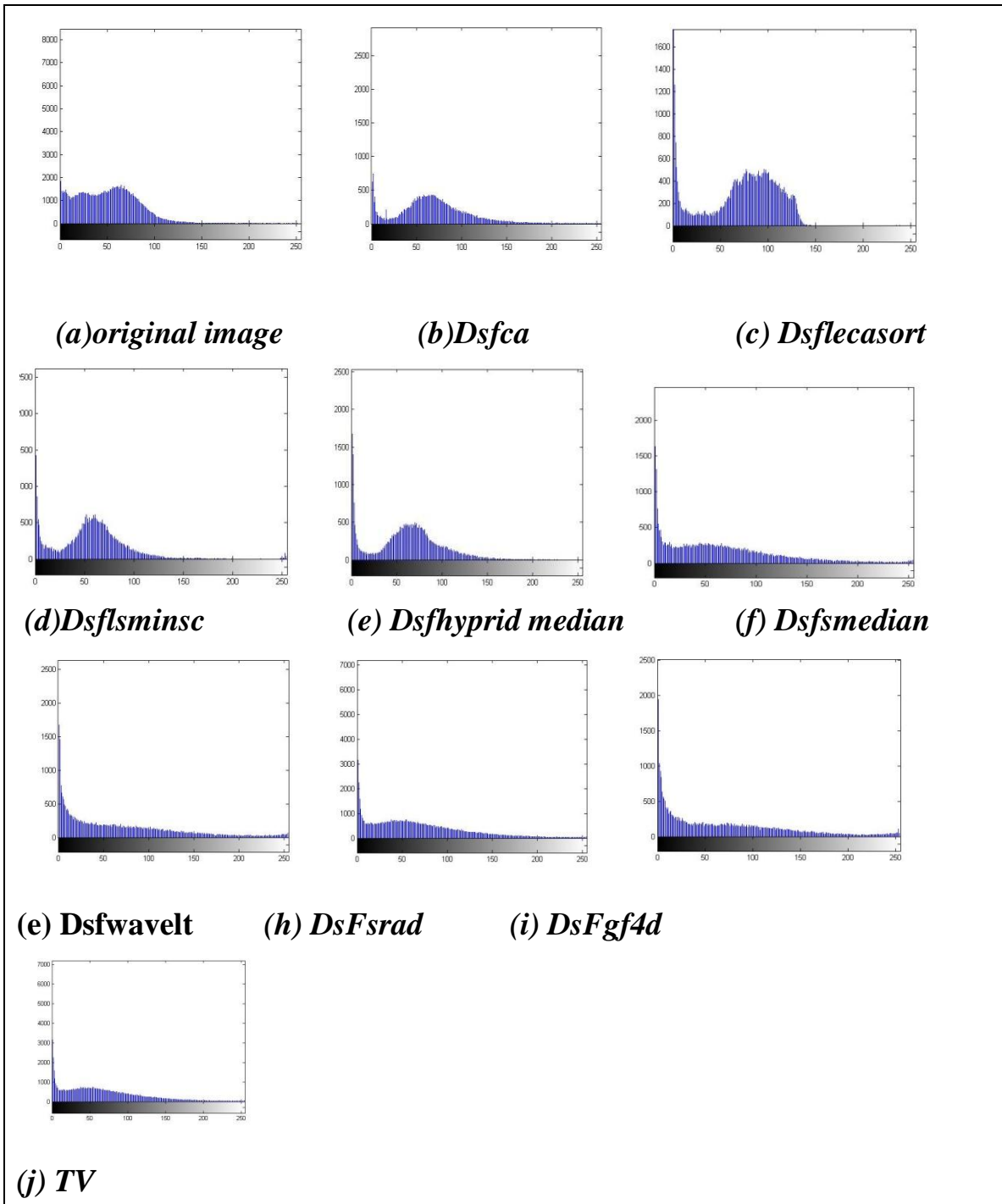


FIGURE 5.8: Histogram result of liver despeckled by various filter on multiplication noise (noise =0.5).

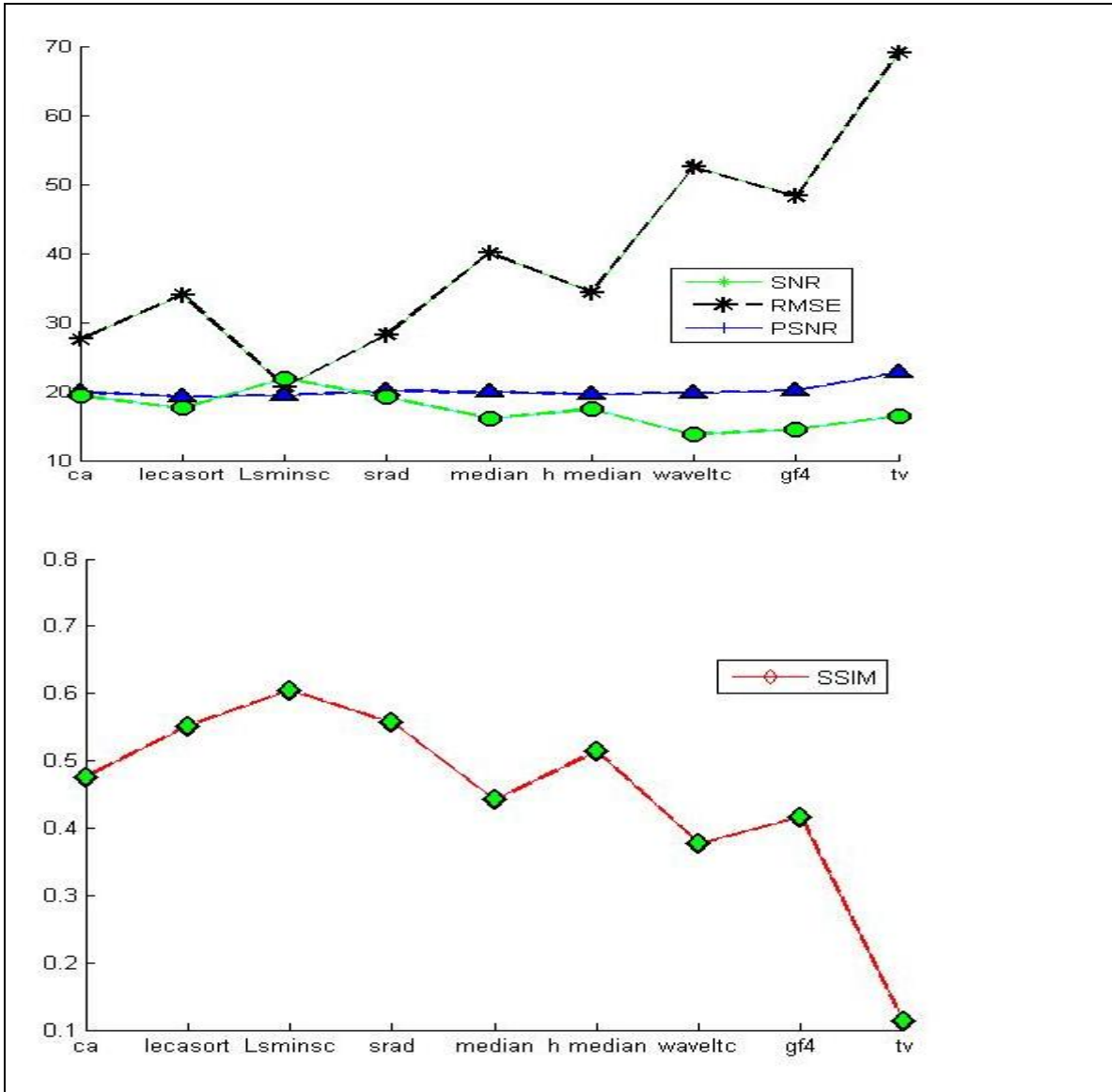


FIGURE 5.9: Performance analysis graph to image quality evaluation metric for kidney image (noise $\sigma_n = 0.5$).

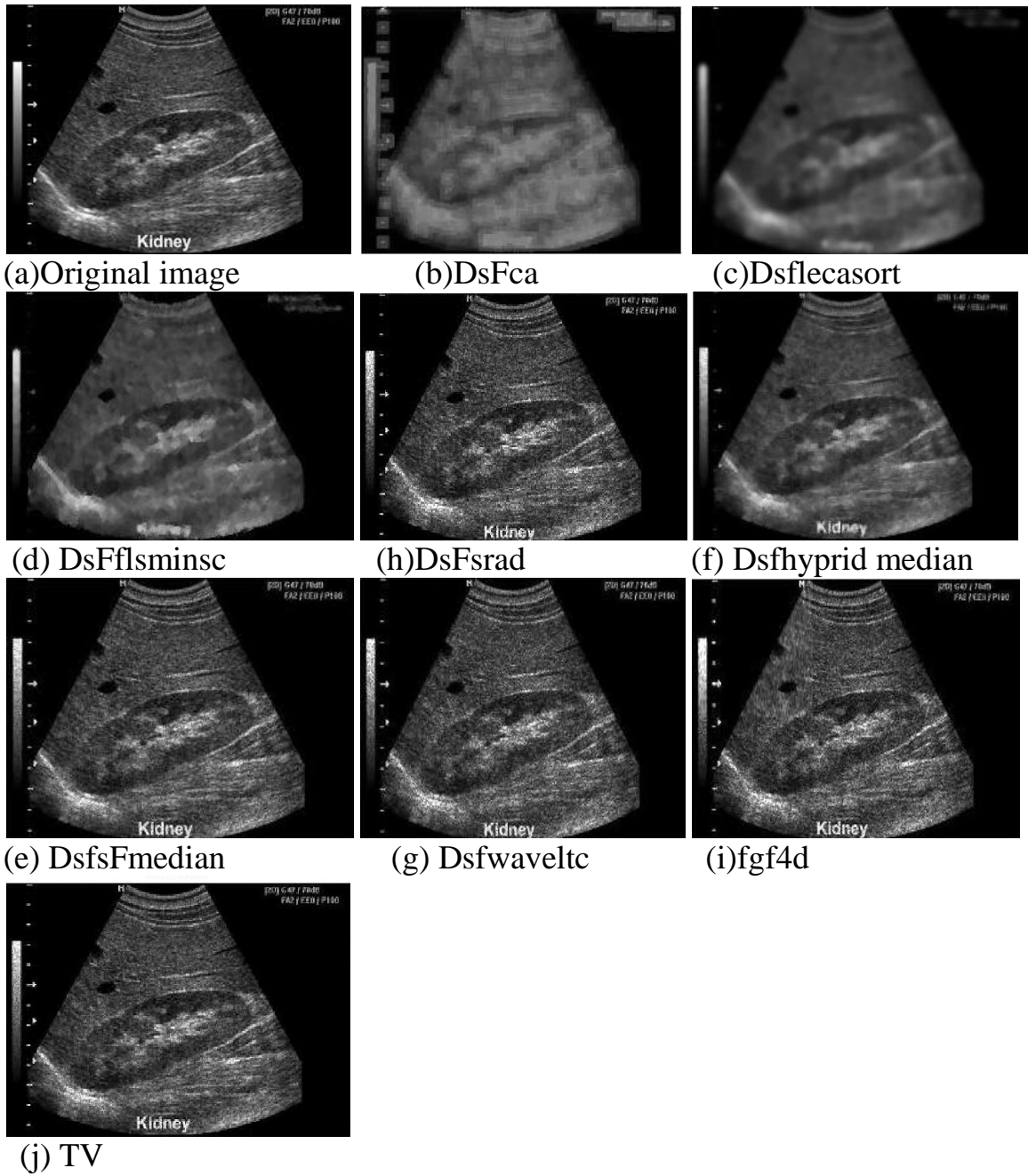


FIGURE 5.10: Results of kidney despeckled by various filter on multiplication noise ($\sigma_n=0.05$).

Table5.4: Image quality evaluation metrics computed for the kidney ($\sigma_n = 0.05$) at statistical measurement of RMSE,PSNR, SNR and SSIM for different filter types.

Types of filter	Images quality metrics			
	RMSE	PSNR	SNR	SSIM
Dsfca	36.9040	16.82838	19.9887	0.4379
Dsflecasort	20.2510	22.0359	19.2885	0.5870
Dsflsminsc	26.8804	19.5761	26.42262	0.6237
DsFsrاد	16.5021	23.8140	19.6425	0.8261
Dsfsmedian	36.1058	17.013	19.5664	0.5081
Dsfhybridmedian	26.1237	19.8241	19.5336	0.6512
Dsfwaveltc	18.7706	22.6953	22.6640	0.7083
DsFgf4	17.868	23.0657	19.6942	0.7283
Tv	13.0290	25.866	22.7882	0.4602

Bold number indicates the best values.

* Signal to- noise ratio (SNR), peak-to-noise ratio (PSNR) ,structural similarity index(SSIM) and root mean square error(RMSE).

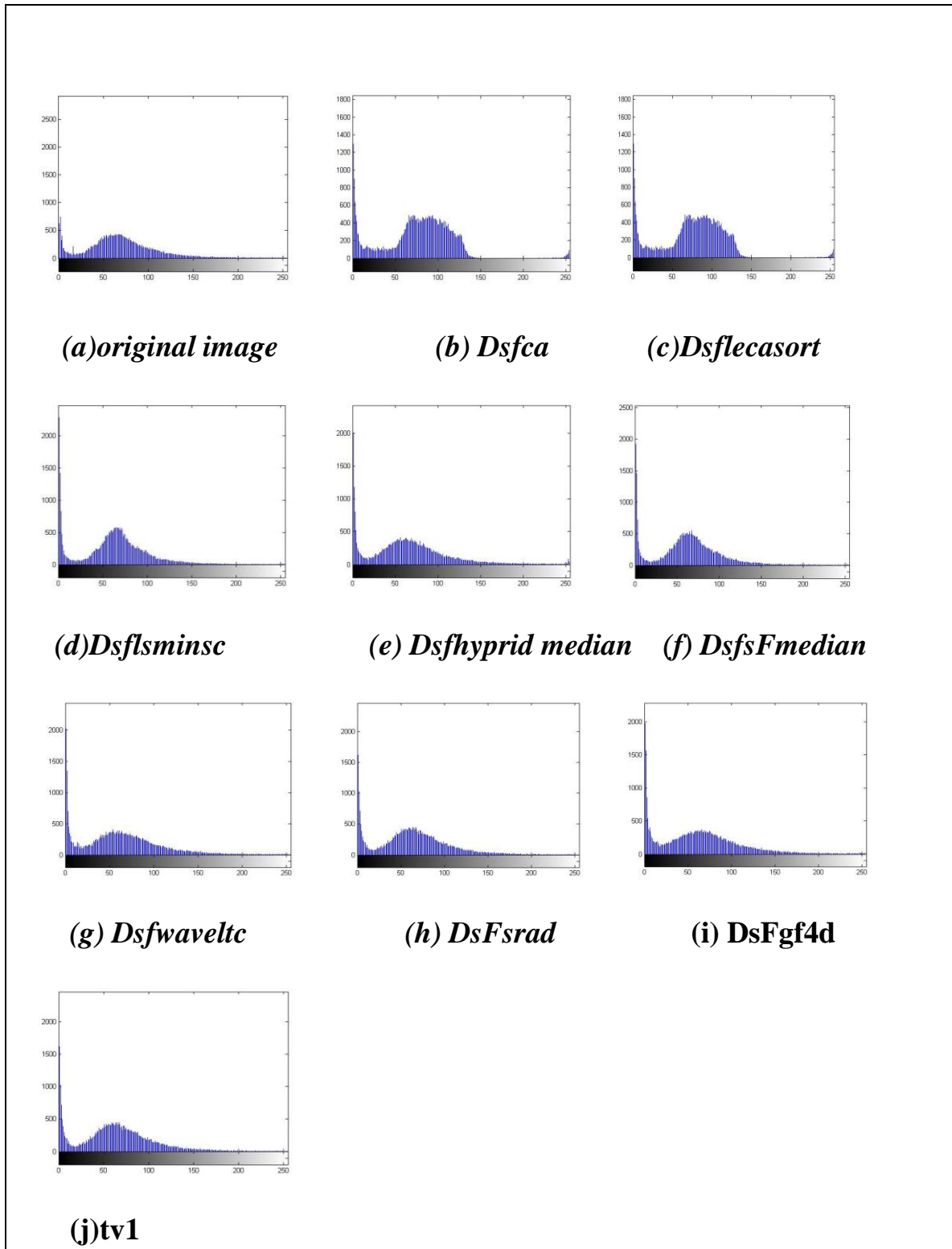


FIGURE 5.11: Histogram result of kidney despeckled by various filter on multiplication noise (noise =0.05).

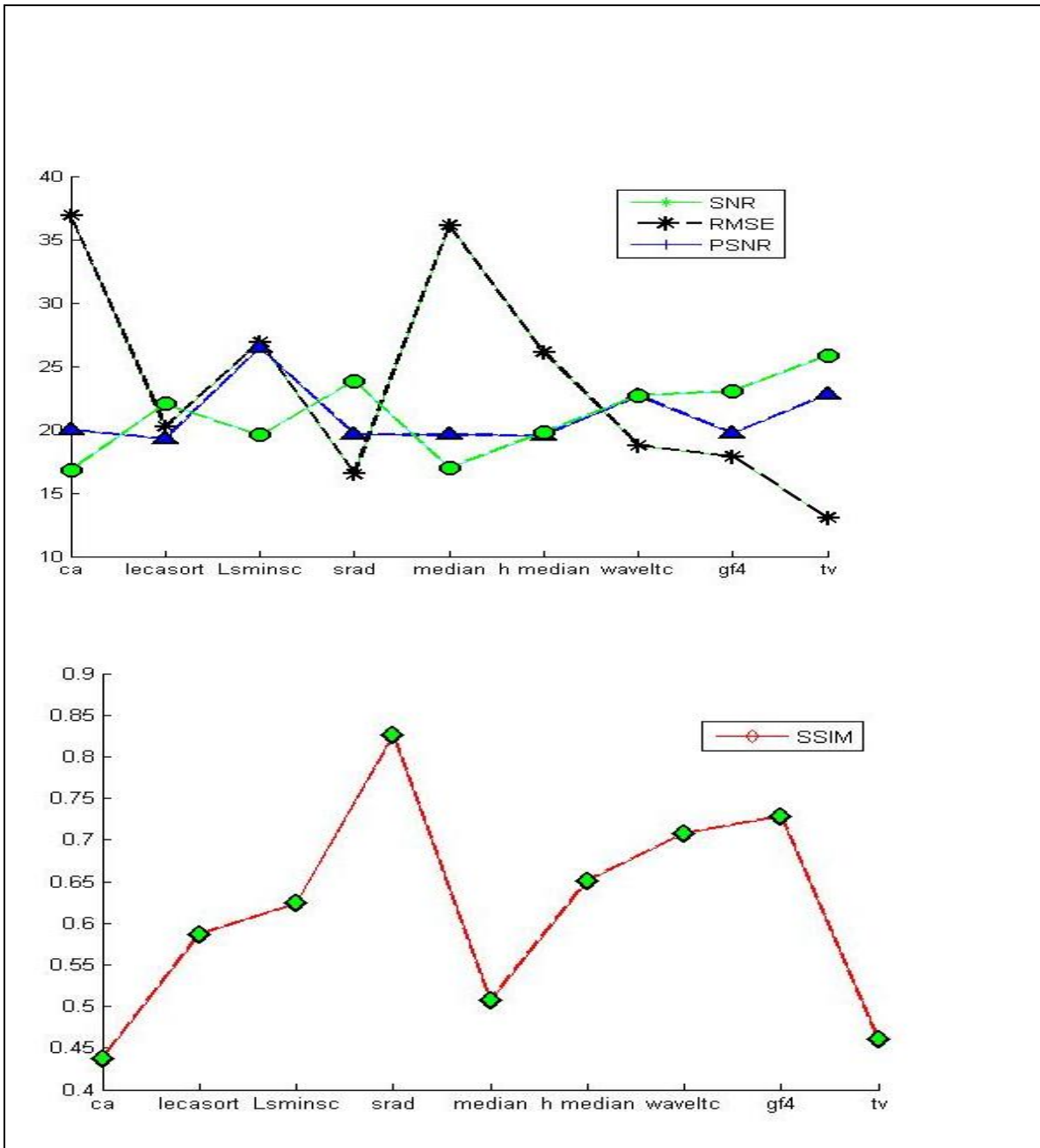


FIGURE 5.12: Performance analysis graph to image quality evaluation metric for kidney image (noise $\sigma_n = 0.05$).



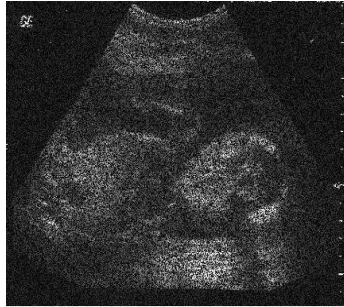
(a)Original image

(b)DsFca

(c)Dsflucasort



(d)DsFflsminsc



(e)DsFsrads



(f) Dsfhybrid median



(g) DsfsFmedian



(h)Dsfwaveltc



(i)DsFgf4d



(j)tv

FIGURE 5.13: Results of fetal despeckled by various filter on multiplication noise ($\sigma_n=0.5$).

Table5.5: Image quality evaluation metrics computed for the fetal ($\sigma_n=0.5$) at statistical measurement of **RMSE,PSNR, SNR** and **SSIM** for different filter types.

Types of filter	Images quality metrics			
	RMSE	PSNR	SNR	SSIM
Dsfca	16.8600	23.6276	18.6609	0.7943
Dsflecasort	14.9404	24.6776	18.4317	0.8259
Dsflsminsc	17.8900	23.1126	18.6075	0.6842
DsFsrاد	16.5964	23.7640	21.2981	0.9354
Dsfsmedian	27.0533	19.504	18.6221	0.66610
Dsfhybridmedian	17.3545	23.3766	18.4595	0.8751
Dsfwaveltc	33.6234	17.6320	18.9558	0.1545
DsFgf4	36.6210	16.890	18.6203	0.5454
Tv	20.9082	21.7585	18.6051	0.7356

Bold number indicates the best values.

* signal-to-noise ratio (SNR), peak-to-noise ratio (PSNR), structural similarity index(SSIM) and root mean square error(RMSE)

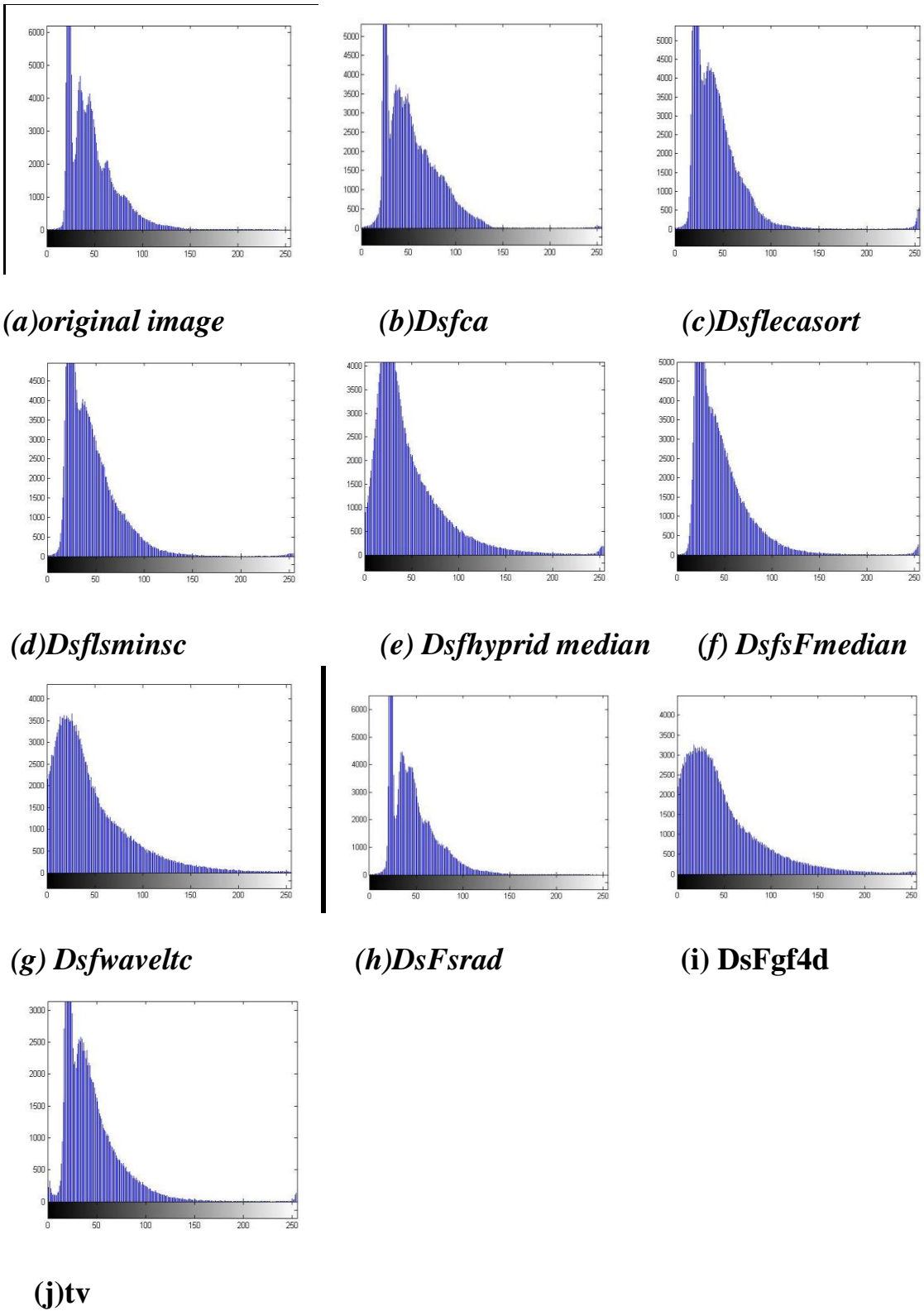


FIGURE 5.14 : Histogram result of fetal despeckled by various filter on multiplication noise(noise =0.5) .

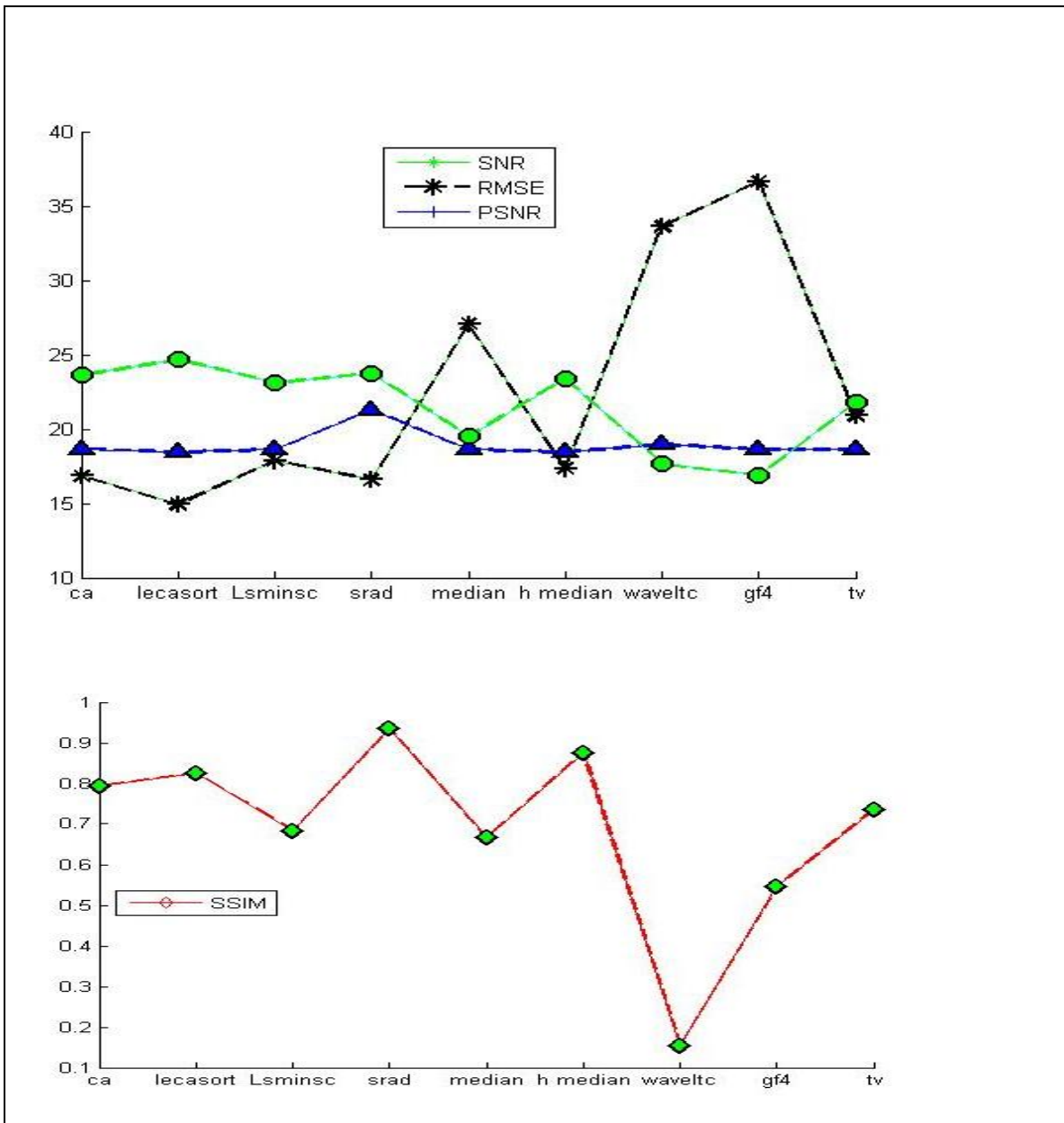


FIGURE 5.15: Performance analysis graph to image quality evaluation metric for fetal image (noise $\sigma_n = 0.5$).

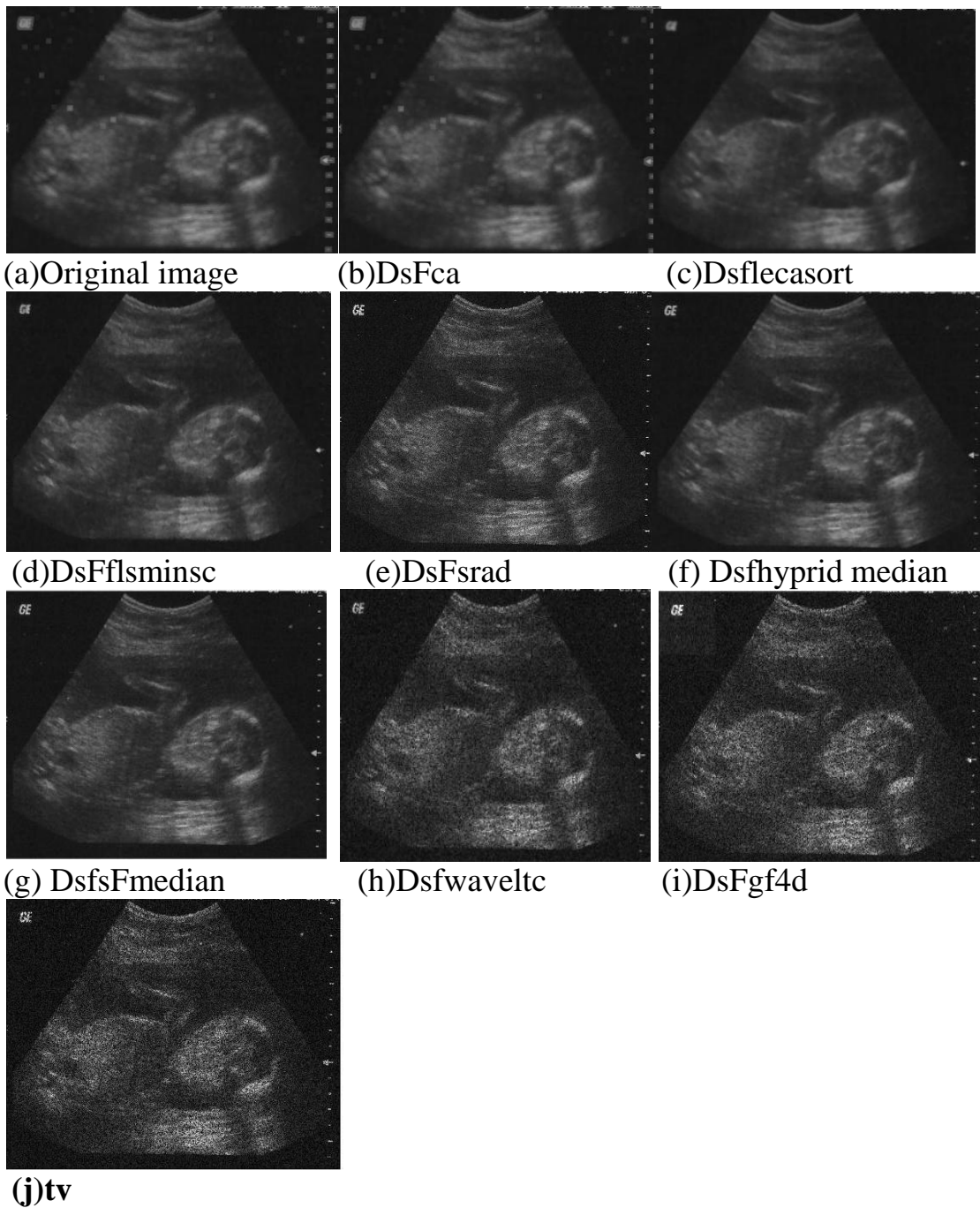


FIGURE5.16 : Results of fetal despeckled by various filter on multiplication noise ($\sigma_n=0.05$).

Table5.6: Image quality evaluation metrics computed for the fetal ($\sigma_n=0.05$) at statistical measurement of **RMSE,PSNR, SNR** and **SSIM** for different filter types.

Types of filter	Images quality metrics			
	RMSE	PSNR	SNR	SSIM
Dsfca	14.5654	24.8983	18.6609	0.7943
Dsflecasort	12.9228	25.9376	18.4317	0.8259
Dsflsminsc	17.9152	23.1004	18.6075	0.6842
DsFsrاد	2.9952	38.6362	21.2981	0.9354
Dsfsmedian	18.8615	22.6533	18.6221	0.66610
Dsfhybridmedian	5.4503	33.4364	18.4595	0.8751
Dsfwaveltc	33.6556	13.6237	18.9558	0.1545
DsFgf4	17.4991	23.3045	18.6203	0.5454
Tv	10.3338	27.8796	18.4407	0.7356

Bold number indicates the best values.

* signal-to-noise ratio (SNR), peak-to-noise ratio (PSNR), structural similarity index(SSIM) and root mean square error(RMSE).

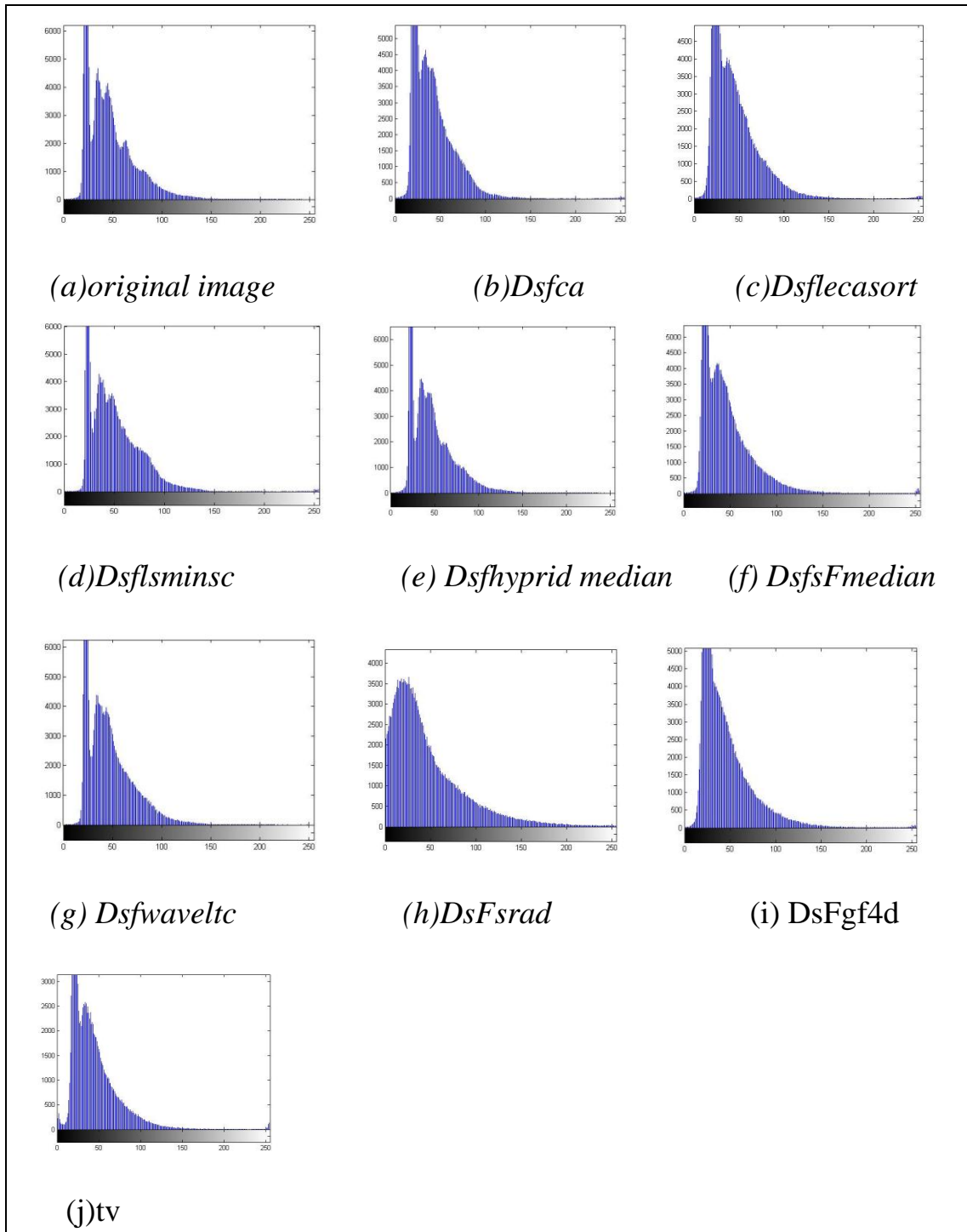


FIGURE 5.17: Histogram result of fetal despeckled by various filter on multiplication noise (noise = 0.05) .

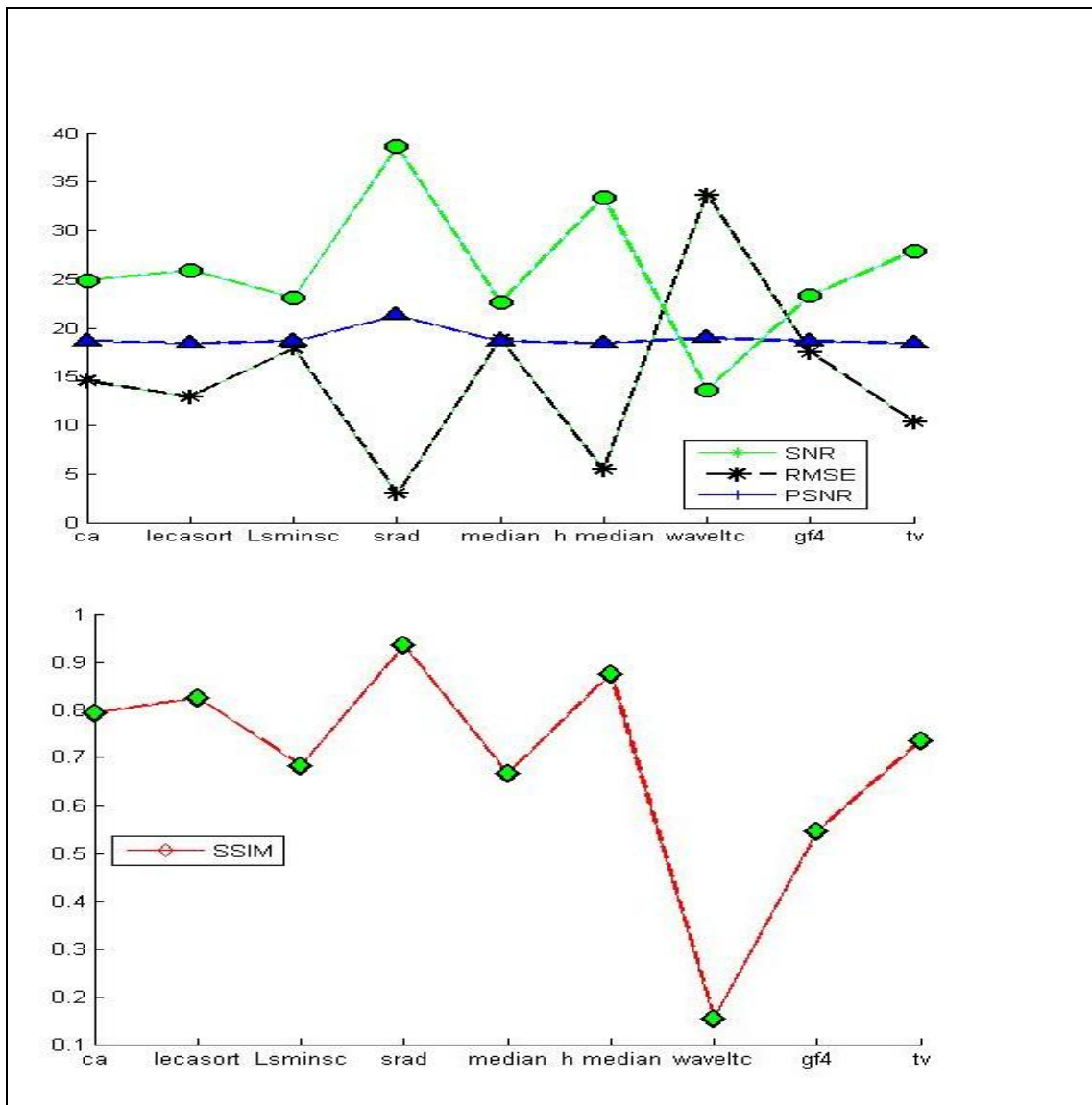
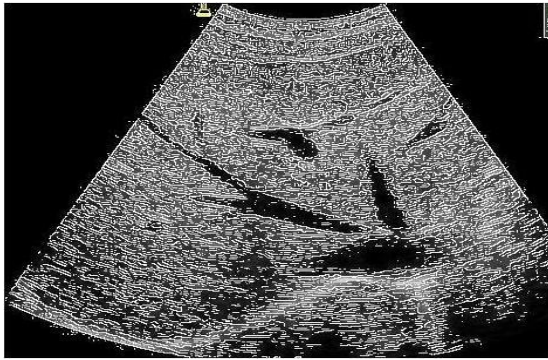
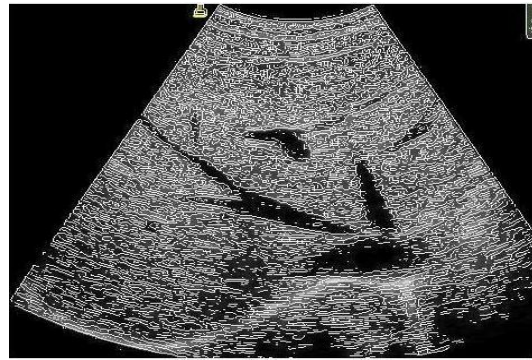


FIGURE 5.18: Performance analysis graph to image quality evaluation metric for fetal image (noise $\sigma_n = 0.05$).

Post processing Result



(a)canny



(b)log



(c)prewitt

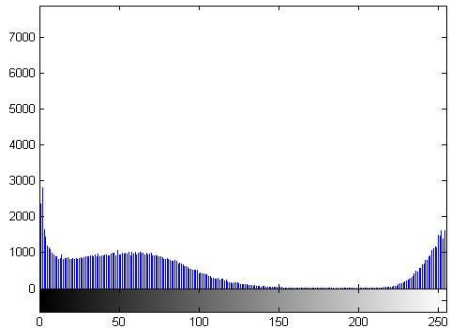


(d)roberts

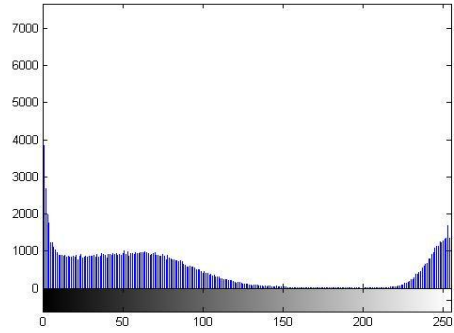


(e)sobel

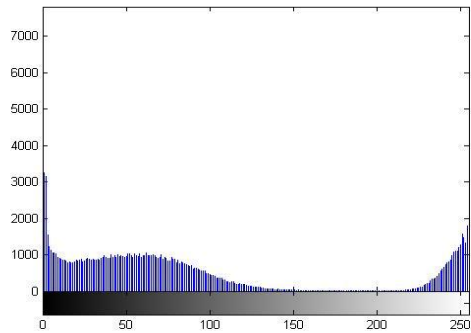
Figure5.19: result of various edge detection operators for original liver image.



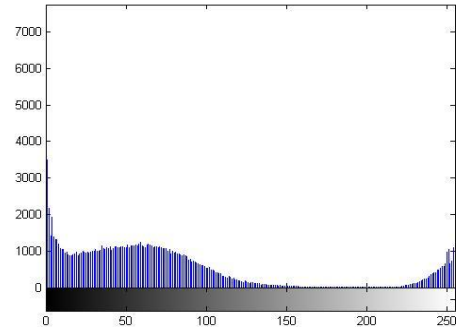
(a)canny



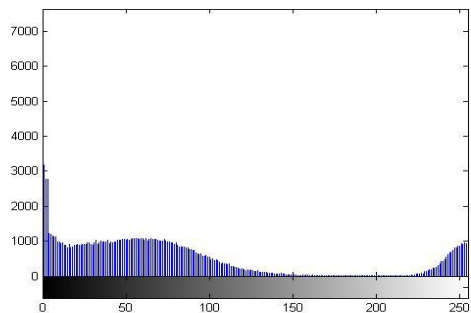
(b)log



(c)prewitt



(d)roberts

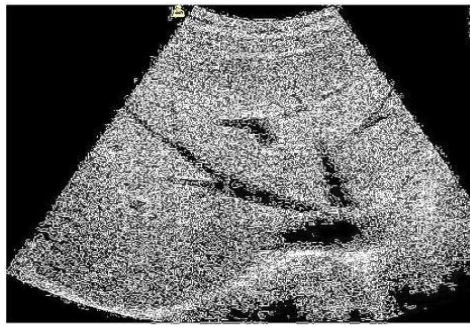


(e)sobel

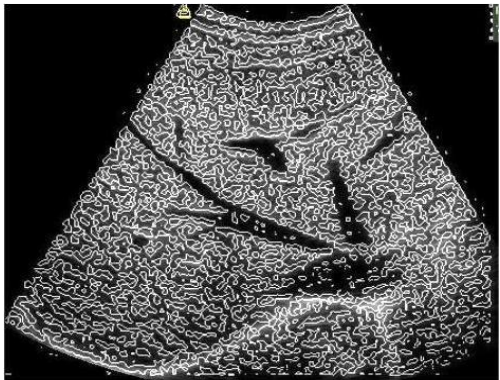
Figure 5.20: histogram result of various edge detection operators for original liver image.



(a)canny



(b)log



(c)prewitt

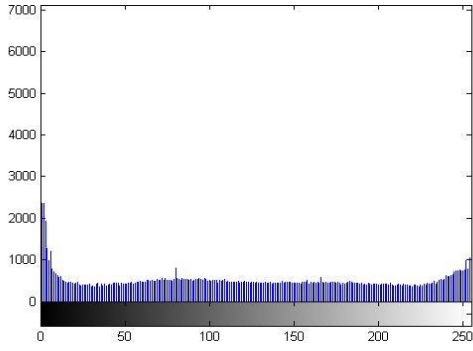


(d)roberts

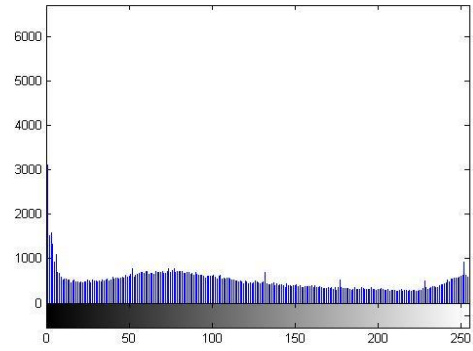


(e)sobel

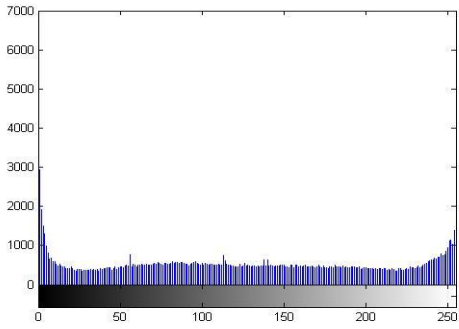
Figure5.21: result of various edge detection operators for despeckling liver image DSFRAD ($\sigma_n 0.5$) .



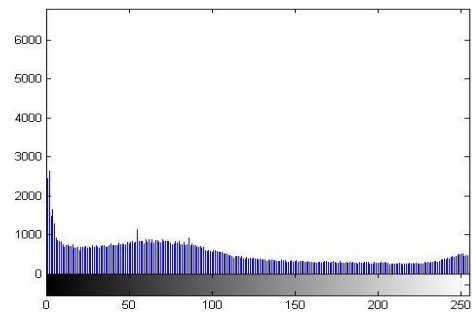
(a)canny



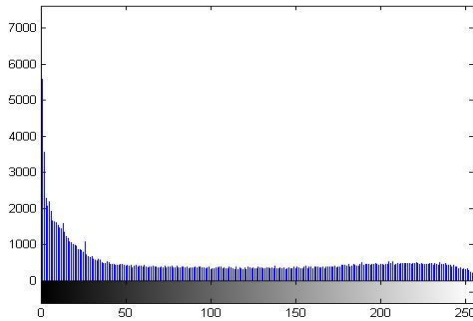
(b)log



(c)prewitt



(d)roberts



(e)sobel

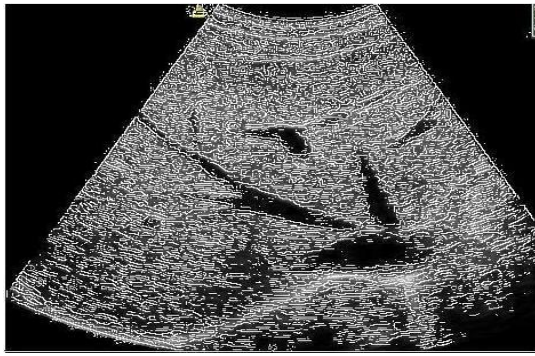
Figure 5.22: histogram result of various edge detection operators for despeckling liver image DSFRAD ($\sigma_n 0.5$).

Table5.7:Image quality evaluation metrics computed for the liver edge detection operators ($\sigma =0.5$) at statistical measurement of RMSE,PSNR SNR and SSIM for different filter types.

	Sobel	Roberts	Prewitt	Log	Canny
RMSE	65.0963	77.1190	74.1670	73.5326	81.8045
PSNR	31.9460	26.7952	27.7343	27.8820	30.4156
SNR	22.3818	22.2017	22.5262	21.5089	21.8489
SSIM	0.5489	0.5253	0.5591	0.5111	0.2735

Bold number indicates the best values.

signal-to-noise ratio (SNR), peak-to-noise ratio (PSNR),structural similarity index(SSIM) and root mean square error(RMSE).



(a)canny



(b)log



(c)prewitt

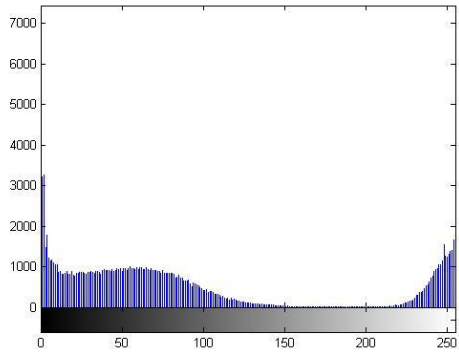


(d)roberts

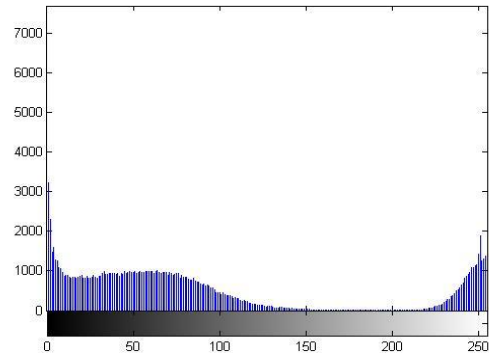


(e)sobel

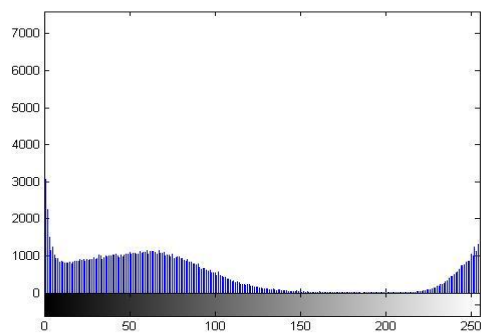
Figure5.23: result of various edge detection operators for despeckling liver image DSFRAD (σ_n 0.05) with.



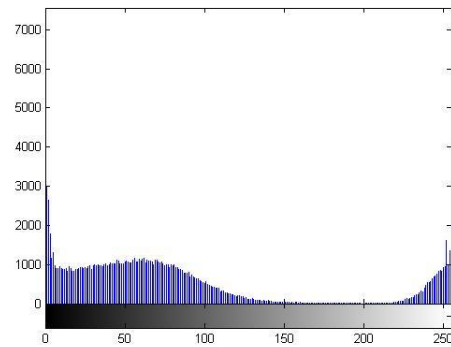
(a)canny



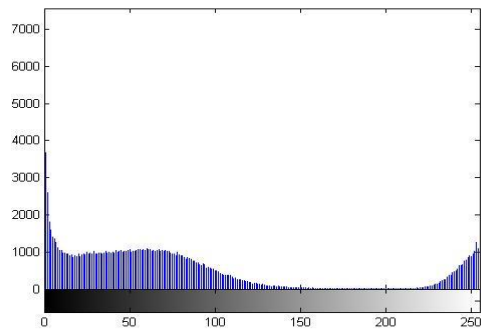
(b)log



(c)prewitt



(d)roberts



(e)sobel

Figure 5.24: histogram result of various edge detection operators for despeckling liver image DSFRAD ($\sigma_n 0.05$).

Table5.8:Image quality evaluation metrics computed for the liver edge detection operators($\sigma_n = 0.05$) at statistical measurement of **RMSE**,**PSNR** **SNR** and **SSIM** for different filter types.

	Sobel	Roberts	Prewitt	Log	Canny
RMSE	70.0777	79.5834	80.1936	76.5068	73.4462
PSNR	30.1181	24.8178	24.4042	27.3503	25.2927
SNR	22.3210	21.9891	22.1829	21.2499	21.7742
SSIM	0.5321	0.2749	0.5802	0.4918	0.2749

Bold number indicates the best values.

signal-to-noise ratio (SNR), peak-to-noise ratio (PSNR), structural similarity index(SSIM) and root mean square error(RMSE).



(a)canny



(b)log



(c)prewitt

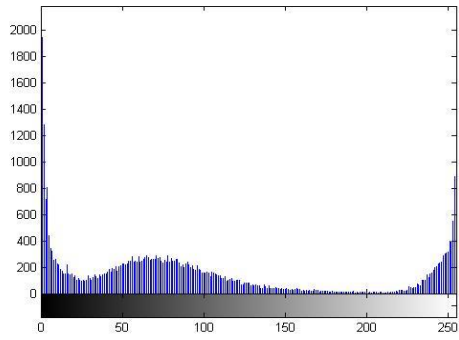


(d)roberts

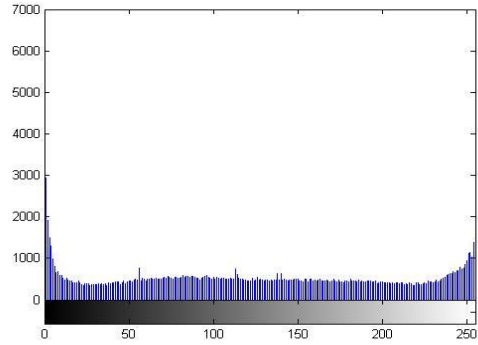


(e)sobel

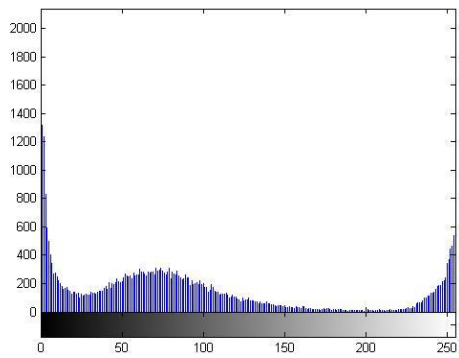
Figure 5.25: result of various edge detection operators to original kidney image.



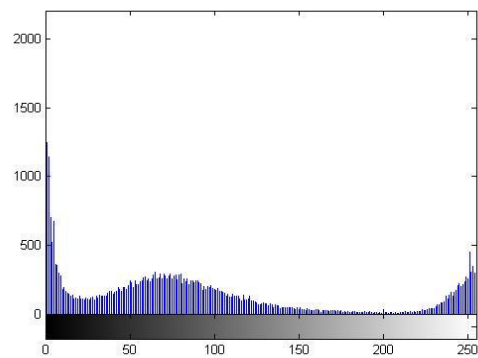
(a)canny



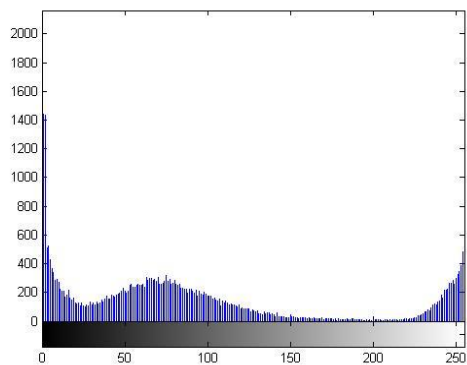
(b)log



(c)prewitt

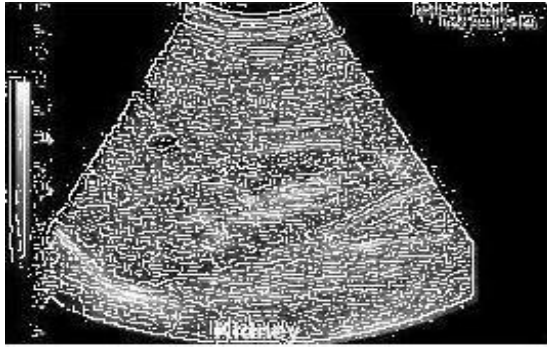


(d)roberts



(e)sobel

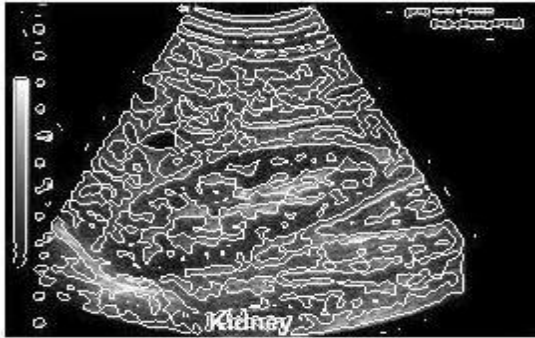
Figure 5.26 : histogram result of various edge detection operators to original kidney image.



(a)canny



(b)log



(c)prewitt

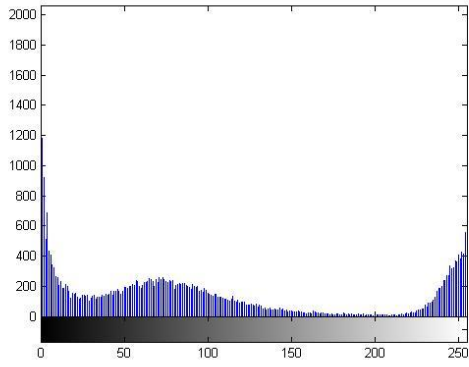


(d)roberts

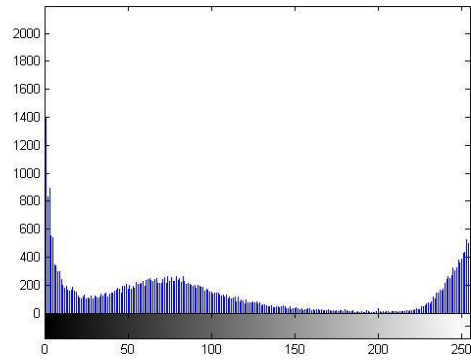


(e)sobel

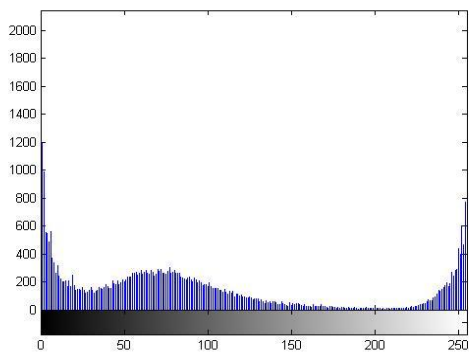
Figure 5.27: result of various edge detection operators for despeckling kidney image DSFRAD ($\sigma_n 0.5$) .



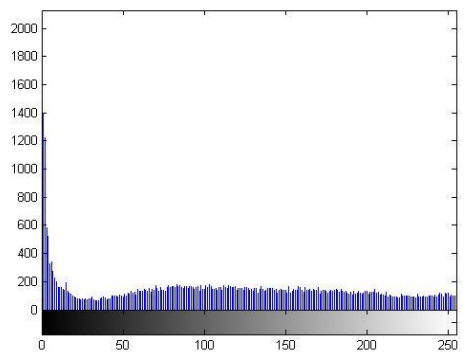
(a)canny



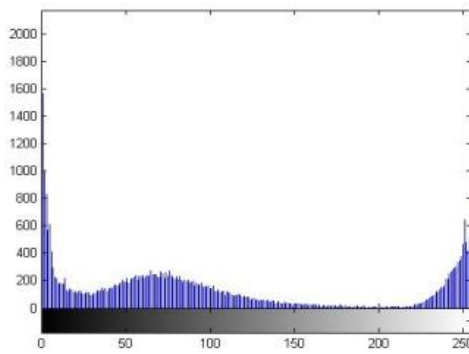
(b)log



(c)prewitt



(d)roberts



(e)sobel

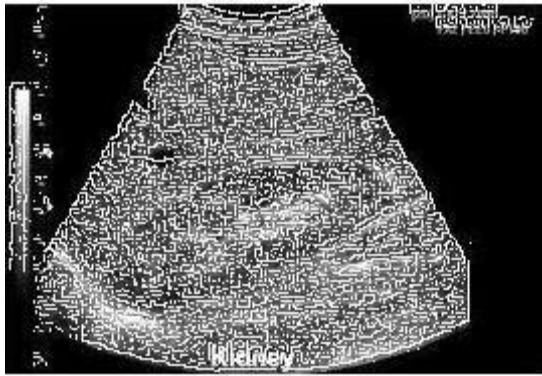
Figure 5.28: histogram result of various edge detection operators for despeckling kidney image DSFRAD ($\sigma = 0.5$).

Table5.9:Image quality evaluation metrics computed for the kidney edge detection operators($\sigma =0.5$) at statistical measurement of **RMSE,MPSNR** **SNR** and **SSIM** for different filter types.

	Sobel	Roberts	Prewitt	log	Canny
RMSE	40.1380	63.198	60.5256	58.7625	50.0830
PSNR	30.8417	24.9924	25.2723	26.2253	31.1325
SNR	22.3173	22.1804	21.9147	21.9780	22.0175
SSIM	0.5635	0.6754	0.6829	0.6637	0.7210

Bold number indicates the best values.

* signal-to-noise ratio (SNR), peak-to-noise ratio (PSNR), structural similarity index(SSIM) and root mean square error(RMSE).



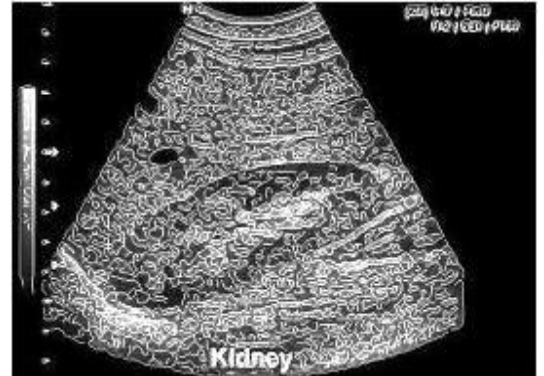
(a)canny



(b)log



(c)prewitt

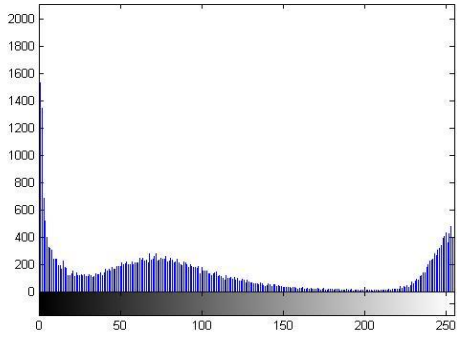


(d)roberts

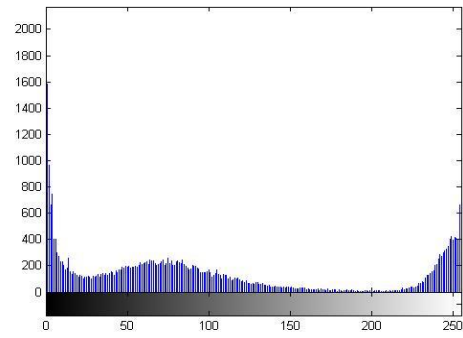


(e)sobel

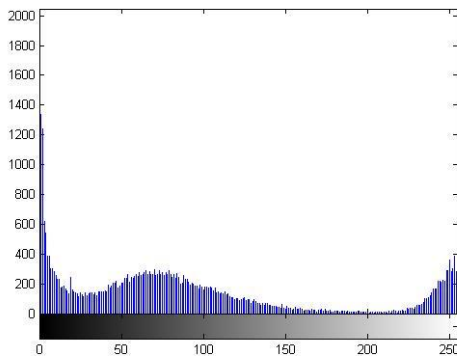
Figure 5.29: result of various edge detection operators to despeckling kidney image DSFRAD ($\sigma= 0.05$) .



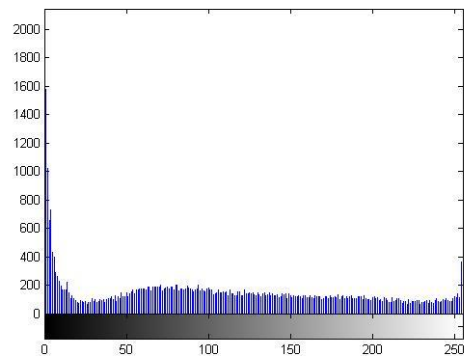
(a)canny



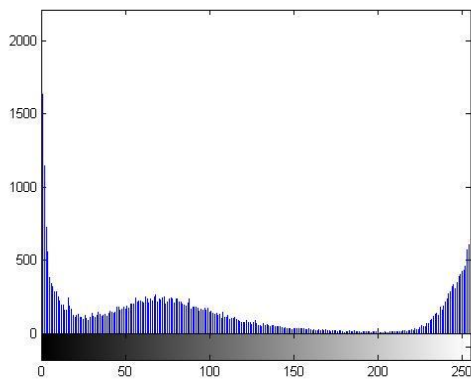
(b)log



(c)prewitt



(d)roberts



(e)sobel

Figure 5.30: histogram result of various edge detection operators for despeckling kidney image DSFRAD ($\sigma= 0.05$) .

Table5.10:Image quality evaluation metrics computed for the kidney edge detection operators ($\sigma= 0.05$) at statistical measurement of **RMSE** ,**PSNR** **SNR** and **SSIM** for different filter types.

	Sobel	Roberts	Prewitt	Log	canny
RMSE	59.0104	60.3044	60.1018	5.83127e+003	48.6312
PSNR	31.4247	25.4272	25.0908	26.7602	30.9248
SNR	22.3237	22.2914	22.1632	22.0254	21.8694
SSIM	0.6989	0.6982	0.5801	0.6712	0.7303

Bold number indicates the best values.

* signal-to-noise ratio (SNR), peak-to-noise ratio (PSNR), structural similarity index(SSIM) and root means square error(RMSE).



(a)canny



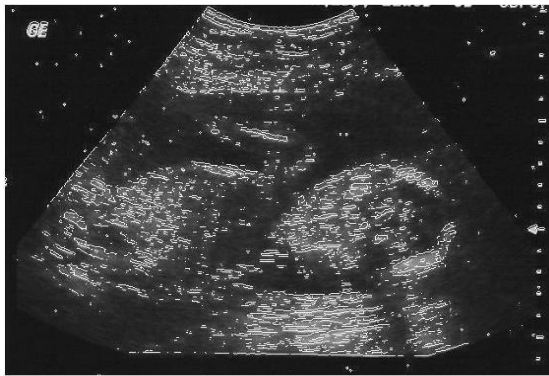
(b)log



(c)prewitt

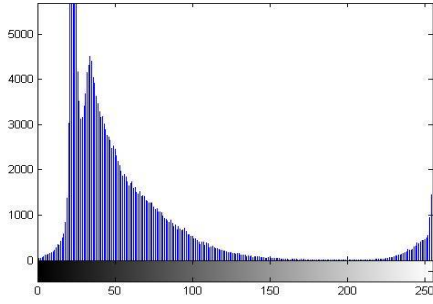


(d)roberts

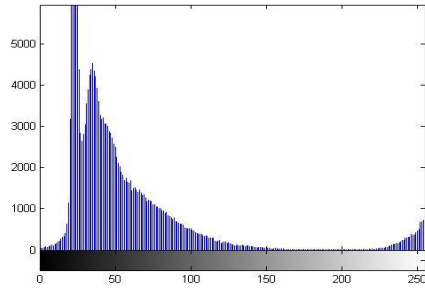


(e)sobel

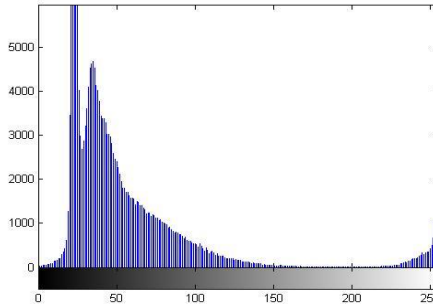
Figure 5.31: result of edge detection operators of original fetal image.



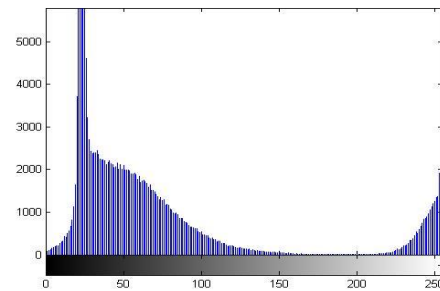
(a)canny



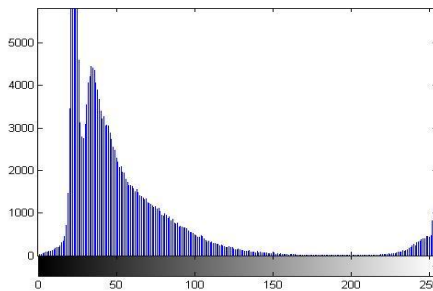
(b)log



(c)prewitt

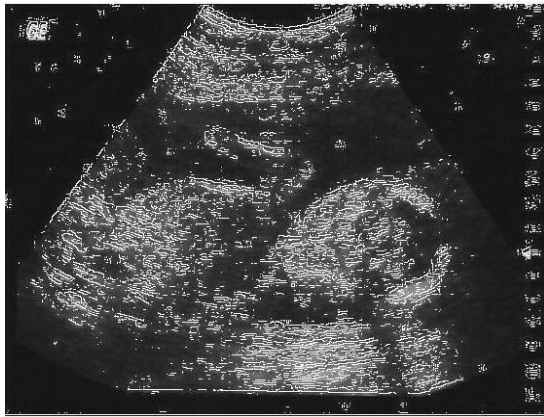


(d)roberts

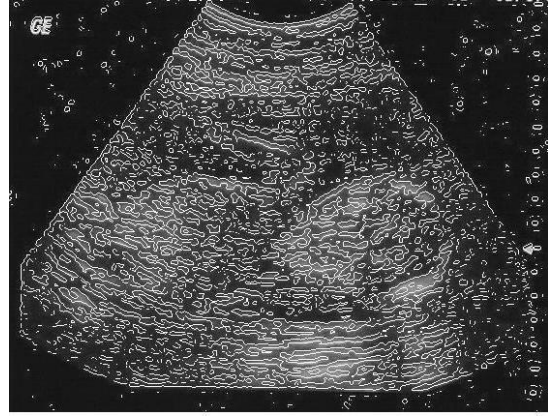


(e)sobel

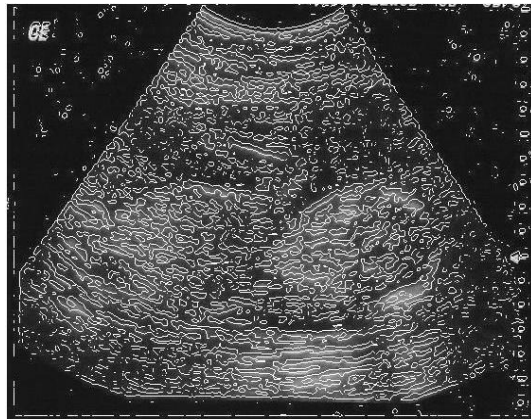
Figure 5.32: histogram result of various edge detection operators for fetal image.



(a)canny



(b)log



(c)prewitt

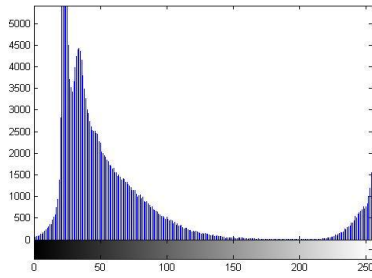


(d)roberts

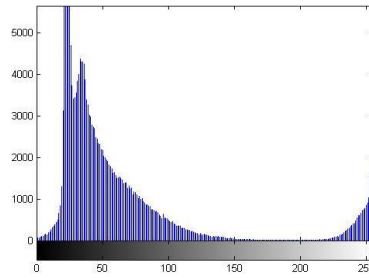


(e)sobel

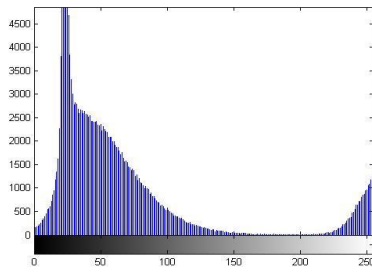
Figure 5.33: result of various edge detection operators for despeckling fetal image DSFRAD ($\sigma_n 0.5$).



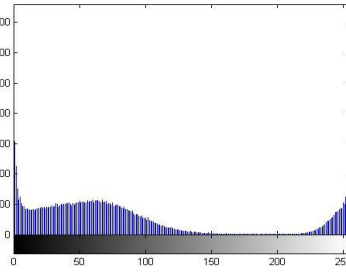
(a)canny



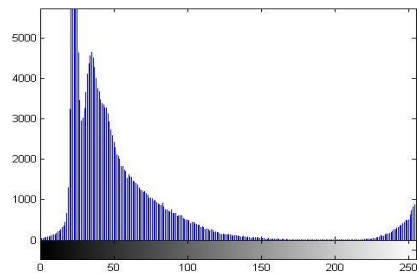
(b)log



(c)prewitt



(d)roberts



(e)sobel

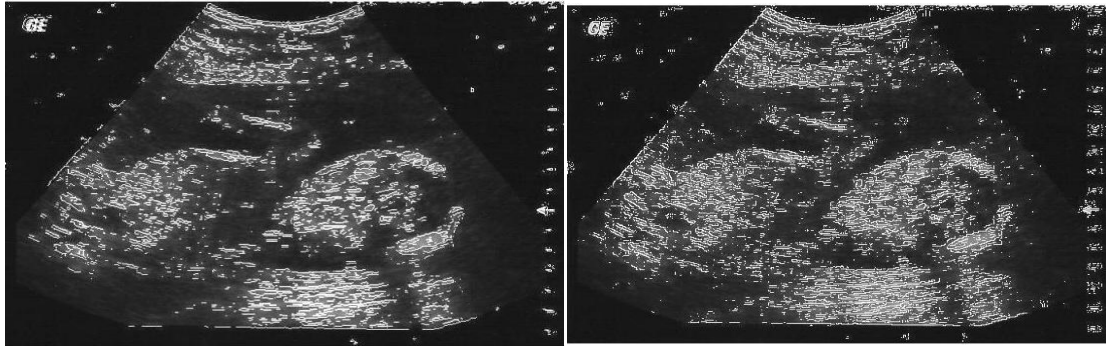
Figure 5.34: histogram result of various edge detection operators for despeckling fetal image DSFRAD ($\sigma=0.5$) .

Table5.11:Image quality evaluation metrics computed for the fetal edge detection operators ($\sigma= 0.5$) at statistical measurement of **RMSE,PSNR SNR** and **SSIM** for different filter types

	Sobel	Roberts	Prewitt	Log	Canny
RMSE	43.1293	49.9187	49.7850	56.8711	62.0039
PSNR	36.1838	33.6026	33.5398	31.6443	30.0035
SNR	20.7438	20.5253	20.5473	20.2557	21.4810
SSIM	0.6346	0.6727	0.5284	0.5415	0.5284

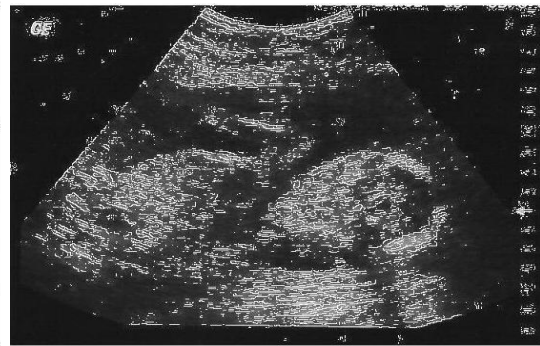
Bold number indicates the best values.

* signal-to-noise ratio (SNR), peak-to-noise ratio (PSNR),structural similarity index(SSIM) and root mean square error(RMSE).



(a)canny

(b)log



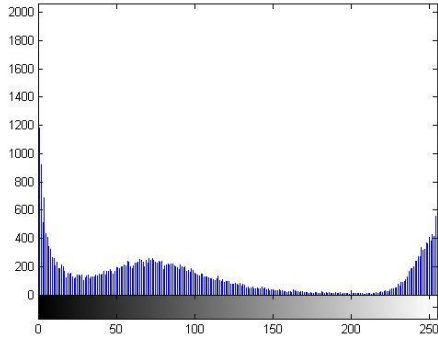
(c)prewitt

(d)roberts

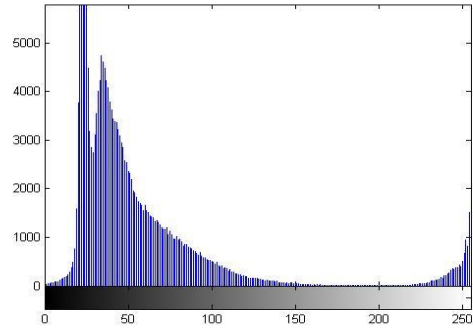


(e)sobel

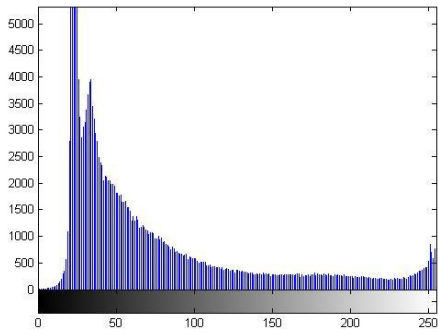
Figure5.35 : result of various edge detection operators for despeckling fetal image DSFRAD ($\sigma= 0.05$).



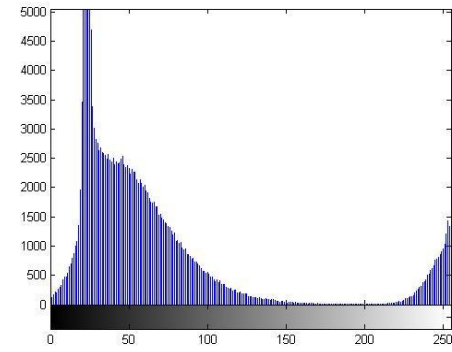
(a)canny



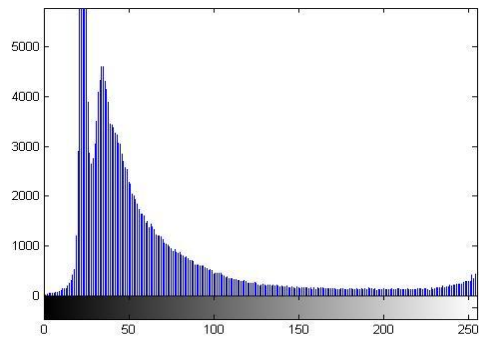
(b)log



(c)prewitt



(d)roberts



(e)sobel

Figure 5.36: histogram result of various edge detection operators for despeckling fetal image DSFRAD ($\sigma= 0.05$).

Table 5.12 : Image quality evaluation metrics computed for the fetal edge detection operators($\sigma=0.05$) at statistical measurement of **RMSE,PSNR ,SNR** and **SSIM** for different filter types.

	Sobel	Roberts	prewitt	Log	Canny
RMSE	40.2484	49.2647	26.0326	74.3152	66.4355
PSNR	39.3039	33.6695	46.5281	37.5989	30.0035
SNR	20.9075	20.7028	20.1487	20.5297	21.5339
SSIM	0.8875	0.6699	0.4936	0.3056	0.4936

Bold number indicates the best values.

* signal-to-noise ratio (SNR), peak-to-noise ratio (PSNR), structural similarity index(SSIM) and root means square error(RMSE).

Most importantly, a despeckle filtering analysis and evaluation framework is proposed for selecting the most appropriate filter or filters for the images under investigation. The filters can be further developed and evaluated at a larger scale, texture analysis, image quality evaluation metrics, and visual evaluation by experts.

From figures 5.1, 5.4, 5.7, 5.10, 5.13, 5.16 show an ultrasound image (a) original image (b) and the despeckled images. In (b) can see that, the linear scaling gray level filter (DsFca) has high degree of blurring and was affect on gray level, because it is compute the mean of all pixels whose difference in the gray level with the intensity (the middle pixel in the moving window) is lower than or equal to a given threshold, (c) Show the result obtained by liner scaling The DsFlecasort filter takes k points of a pixel neighborhood, which are closest to the gray level of the image at point (the middle point in the moving window), including]. It then assigns the mean value of these points to the pixel, (d) show the result of *DsFlsmisc* is a 2D filter operating in The middle pixel of the neighborhood is substituted with the average gray level

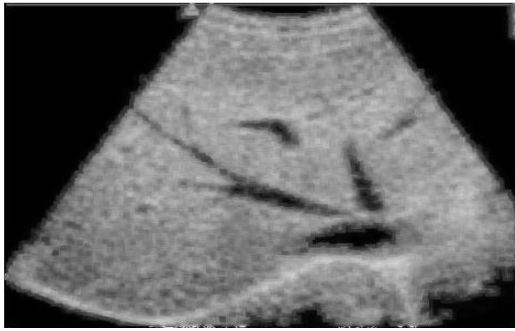
of the mask with the smallest speckle index which, for log-compressed images, figure (e) show The result of hybrid median filter (Dsfhybermedian) that given better edge preserving characteristics than normal median filter, (f) show the result obtained by median despeckle filter, which don't able to remove the speckle and produced blurred edges in the filtered image, (g) the result through wavelet despeckle filtering perceived that it's moderate in order of variance decreasing but execute to decrease the contrast, (h) show the result of speckle reducing anisotropic diffusion filtering (srad), it is better for preserves the edges as a comparison with the other despeckle filtering techniques and subjectively has good result, and referred to evaluated metrics, it was also given bad results, (i) although the result obtained by geometric despeckle filter (DsFgf4d) given poor performance for removing the speckle noise from the ultrasound image, it is lead to increasing the contrast significantly of the image. (J) show the result obtained by total variation despeckle filter (TV) methods. We see that most of the unwanted details haven't been removed efficiently, whilst preserving important details such as edges.

From table 5.1, 5.2, 5.3, 5.4, 5.5, 5.6 tabulates the image quality evaluation contains the metric result of filters under study, The best visual results were obtained for the filters SRAD, Dsflecasort and DsFca because with higher SNR and PSNR and lower RMSE and Best values for the SSIM, but visually, smoothed the image. Loosing subtle details are been observed.

From figure 5.21, 5.23, 5.26, 5.28, 5.31, 5.33 image edge detection operators (a) canny , (b) laplacian of gaussian , (c)prewitt , (d) robert and (e) sobel were applied for image noise (0.5)and (0.05).

From table5.7, 5.8, 5.9, 5.10,5.11,5.12 tabulates the(IMQS) contain the metrics result of edge detection,the best visual results well obtain for the sobel ,canny edge detection because with higher SNR and PSNR and lower RMSE and Best values for the SSIM.

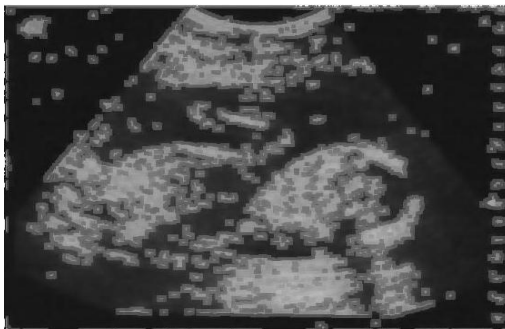
Hybrid technique



(a)liver(0.5)



(b) liver(0.05)



(c) fetal (0.5)



(d) fetal (0.05)

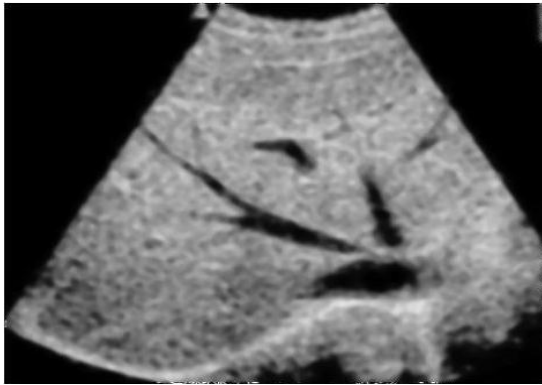


(e) kidney(0.5)

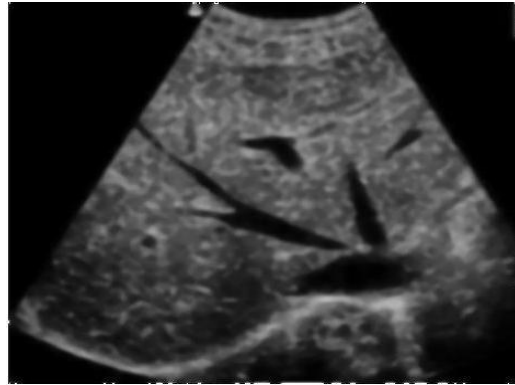


(f) kidney(0.05)

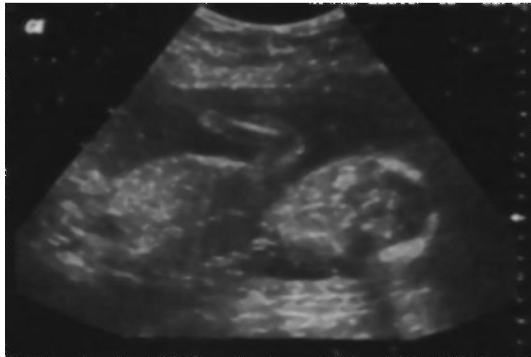
FIGURE 5.37: Result image Hyperid technique by use Linear Scaling Filtering .



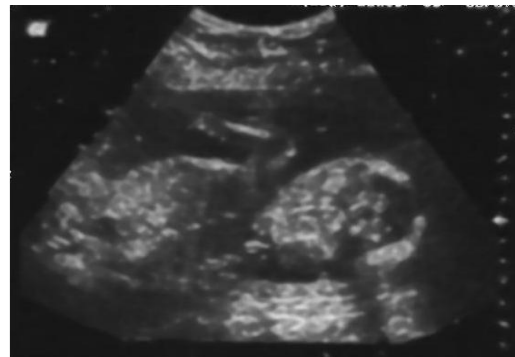
(a)liver(0.5)



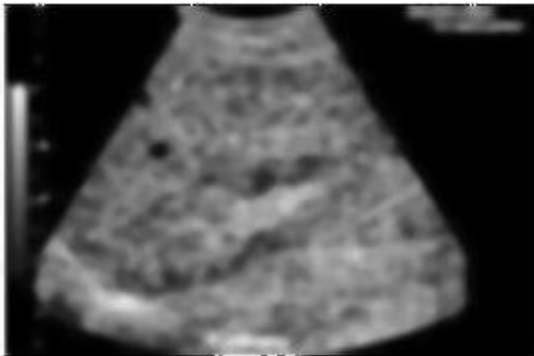
(b) liver(0.05)



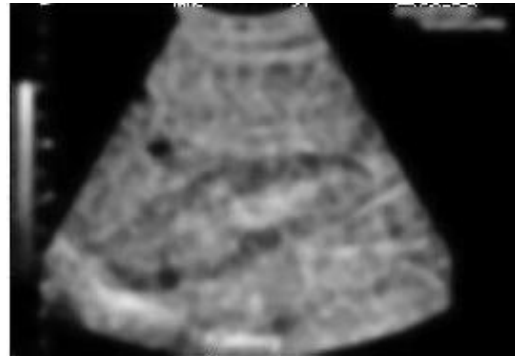
(c) fetal (0.5)



(d) fetal (0.05)

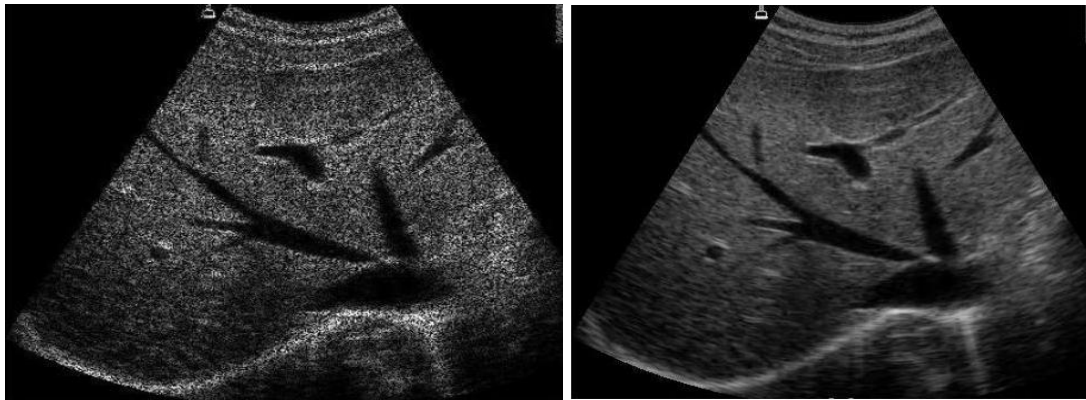


(e) kidney(0.5)



(f) kidney(0.05)

FIGURE 5.38: Result image Hyperid technique with Linear Scaling(NeighborHood Averaging)Filtering .



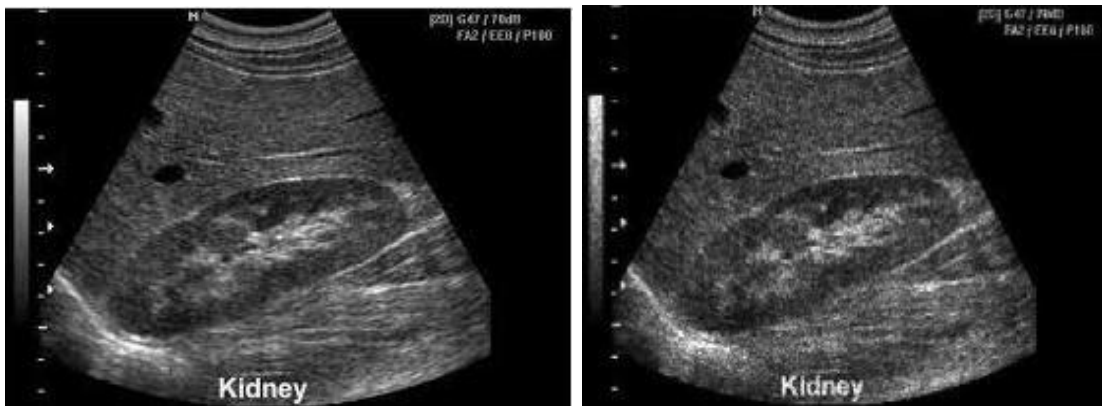
(a)liver(0.5)

(b) liver(0.05)



(c) fetal (0.5)

(d) fetal (0.05)



(e) kidney(0.5)

(f) kidney(0.05)

FIGURE5.39: Result image Hyperid technique by use Anisotropic Diffusion Filtering Filtering .

Table 5.13: Image quality evaluation metrics computed Hyperid technique by use Linear Scaling Filtering(FCA) , Anisotropic Diffusion Filtering(Rad)and Linear Scaling(NeighborHood Averaging)Filtering (sort) statistical measurement of **RMSE,PSNR SNR** and **SSIM**.

IMQs	Liver(0.5)			Fetal(0.5)			Kidney(0.5)		
	FCA	Sort	Rad	FCA	sort	Rad	FCA	sort	Rad
RMSE	43.485 3	41.737 3	88.244 7	43.312 8	38.449 3	44.077 6	72.279 6	86.880 6	86.880 6
PSNR	46.364 2	47.187 1	47.187 1	46.442 4	48.824 6	46.092 4	36.200 6	32.520 7	32.520 7
SNR	20.135 7	22.377 1	21.414 2	20.169 7	19.879 5	19.680 7	15.721 7	21.189 3	21.189 3
SSIM	0.3344	0.3756	0.2624	0.5414	0.6011	0.5811	0.2302	0.3405	0.3405

Bold number indicates the best values.

* Signal -to- noise ratio (SNR), peak-to-noise ratio (PSNR), structural similarity index(SSIM) and root mean square error(RMSE).

*Linear Scaling Filtering(FCA) , speckle reduction Anisotropic Diffusion Filtering(Rad)and Linear Scaling(NeighborHood Averaging)Filtering(sort).

Table 5.14: Image quality evaluation metrics computed Hyperid technique by use Linear Scaling Filtering(FCA) , Anisotropic Diffusion Filtering(Rad)and Linear Scaling(NeighborHood Averaging)Filtering (sort) statistical measurement of RMSE,PSNR SNR and SSIM.

IMQs	Liver(0.05)			Fetal(0.05)			Kidney(0.05)		
	FCA	sort	Rad	FCA	sort	Rad	FCA	sort	Rad
RMSE	68.126 4	64.887 2	71.898 1	35.245 0	34.835 9	41.403 5	72.34 03	68.111 3	86.20 66
PSNR	37.387 3	38.363 5	36.310 0	50.564 9	50.798 4	47.344 1	36.18 38	37.388 5	32.67 65
SNR	16.237 1	20.996 5	20.689 5	21.960 1	20.047 1	19.679 5	15.71 44	22.085 9	21.54 22
SSIM	0.3024	0.3321	0.3164	0.6026	0.6366	0.5976	0.250 3	0.3449	0.315 0

Bold number indicates the best values.

* Signal -to- noise ratio (SNR), peak-to-noise ratio (PSNR), structural similarity index(SSIM) and root mean square error(RMSE).

*Linear Scaling Filtering(FCA) , Anisotropic Diffusion Filtering(Rad)and Linear Scaling(NeighborHood Averaging)Filtering(sort).

From figures 5.37,5.38,5.39 implemented to three best despeckled filter Linear Scaling Filtering(FCA) , Anisotropic Diffusion Filtering(Rad)and Linear Scaling(NeighborHood Averaging)Filtering(sort). From table 5.13,5.14 tabulates the(IMQS) contain the metrics visual results well obtain for the Linear Scaling Filtering(FCA) , Anisotropic Diffusion Filtering(Rad)and Linear Scaling(NeighborHood Averaging)Filtering(sort). we find the best filter (hybrid technique (SO_SORT) get best result than normal one because with higher SNR and PSNR and lower RMSE and Best values for the SSIM , but visually, smoothed the image. Loosing subtle details are been observed .denoise the image and preserve feature .

Concolusion :

The use of filter in Digital Image Processing improves the image to a great extent. Mainly in the case of presence of Speckle noise, filtering is very much required in order to improve the diagnostic examination and also to improve the efficiency of post processing techniques like segmentation. Despeckle filtering is an important operation in the enhancement of ultrasonic imaging. In this research linear scaling gray level filter(DsFca),geometric despeckle filter(DsFg4d),median filter(Dsfmedian),hyper median filter (Dsfhypermedian),homogenous mask area (Dsflminsc) speckle reducing anisotropic diffusion(srad),wavelet filter (Dsfwavelet)and total variation denoising (TVD), Linear Scaling(Neighborhood Averaging)Filtering(Dsflcasort);edge detection sobel ,Robert ,prewitt , lablacian of gauosian and canny have been implemented could be used successfully for the processing of these images.

Initial findings show promising results from several filters, edge detection operators and different clinical images are required to evaluate the performance of the hybrid technique . Other filtering methods may also be studied to compare with these hybrid technique. we can say the sobel edge detection hybrid with lecasort filter (SO_SORT)is best one are noted to be effective in suppressing speckle noise than other filtering techniques, both objectively and subjectively , not only remove speckle but also preserve the details of the image, and preserves the edge properties .

The optimization of proposed "sobel edge detection with SORT" is obtained. With the join SO_SORT technique have demonstrated more robust estimation and more flexibility over other filters.In the evaluation in several image applications including image interpolation and impulsive noise reduction, both quantitative and qualitative comparison showed that the SO_ SORT exhibit improved performance and merit further attention.

In this project, The proposed method sobel edge detecthin SORT speckle filtering (SO_SORT) takes full advantage of combine and modify filters to reduce speckle noise .Experimental results not only to enhancement of those filters but to obtain filters which capable to get a good result referred to quality evaluation metric. While , subjectively, can be used in diagnostic and therapeutic terms .

6.2 Recommendation:

- 1- For edge detection, the thresholds can be taken in the considered to enhance edge detection
- 2- Use Edge Preservation Factor (EPF) as one of Image Quality Evaluation Metrics to evaluate ability of the filter edge preservation.

Reference

- [1]- <http://www.ece.mcmaster.ca/~xwu/ultrasound> , 3 - 2015.
- [2]- <http://41.223.201.246/videoplayer/Lecture6-US.pdf> ,3-2015.
- [3] http://www.online_scienc.com.
- [4] George Saddik, Ph.D, by University of California, Los Angeles, CA ,Bioengineering Department, Ultrasound Imaging System, Feb. 9th 2015.
- [5] S.Kalaivani Narayanan and R.S.D.Wahidabanu,by Dhanalakshmi Srinivasan Engineering College, Government College of Engineering Perambalur, Salem, Tamil Nadu, India , Vol. 2, No.3, September 2009.
- [6]- Banazier A. Abraham and Yasser M. Kadah, by Biomedical Engineering Department, Cairo University, Giza, Egypt, Comparative Evaluation of Despeckle Filtering Techniques In Medical Ultrasound Imaging.
- [7] - Jens E. Wilhjelm, Andreas Illum, Martin Kristensson and Ole Trier, “Medical diagnostic ultrasound physical principles and imaging”, By Andersen Biomedical Engineering, DTU Elektro Technical University of Denmark, 2 October 2013.
- [8]- K. Karthikeyan , Dr. C. Chandrasekar, “Speckle Noise Reduction of Medical Ultrasound Images using Bayesshrink Wavelet Threshold”, may 2012.
- [9] Christos P. Loizou by Intercollege, Cyprus ,Constantinos S. Pattichis by University of Cyprus, Despeckle Filtering Algorithms and Software for Ultrasound Imaging.
- [10] Arpit Singhal, Mandeep Singh, International Journal of Soft Computing and Engineering (IJSCE) Speckle Noise Removal and Edge Detection Using Mathematical Morphology, November 2011.
- [11] HUM YAN CHAI , LAI KHIN WEE , EKO SUPRIYANTO, Department of Clinical Science and Engineering ,Faculty of Health Science and Biomedical Engineering Universiti Teknologi Malaysia UTM Skudai, 81310 Johor, MALAYSIA, Faculty of Computer Science and Automation Institute of Biomedical Engineering and Informatics Technische Universität Ilmenau, 98684, Ilmenau ,GERMANY, Edge Detection in Ultrasound Images Using Speckle Reducing Anisotropic Diffusion in Canny Edge Detector Framework.
- [12] Indrajeet K umar, Jyoti Rawat and Dr. H.S. Bhadauria, by International Journal of Computer Science and Mobile Computing, A CONVENTIONAL STUDY OF EDGE DETECTION TECHNIQUE IN DIGITAL IMAGE PROCESSING, IJCSMC, April 2014.
- [13] <http://www.homepages.inf.ed.ac.uk>.

[14]- Ivan Selesnick , “Total variation denoising (an MM algorithm)”
September 10, 2012, Last edit: March 17, 2014.